Gas Hydrate Growth Kinetics

Experimental Study Related to Effects of Heat Transfer

by

Remi-Erempagamo Tariyemienyo Meindinyo

Thesis submitted in partial fulfillment of
the requirements for the degree of
DOCTOR OF PHILOSOPHY
(PhD)

Faculty of Science and Technology
Department of Petroleum Engineering
2017

University of Stavanger
N-4036 Stavanger
NORWAY
www.uis.no

ISBN: 978-82-7644-700-2
ISSN: 1890-1387
PhD Thesis No. 335

Thanks be to Jehovah God

To my family; especially my parents and my lovely siblings
for all their supports and motivation

and

In memory of Sister Preye Dumofete and Brother Ebinabo Meindinyo
(Peace be upon them)

Preface

This dissertation is submitted in partial fulfillment of the requirements for the degree of PhD (Doctor of Philosophy) in Petroleum Engineering at University of Stavanger, Norway. The thesis presents the results of the research work conducted at Department of Petroleum Engineering, University of Stavanger (UiS) from December 2012. The outcome of this work is given through 2 papers presented at the International Conference on Gas Hydrates (2014), 1 paper published in the Journal Energy&Fuels (2015), 2 papers presented and published in the Proceedings of the 34th International Conference on Ocean, Offshore and Arctic Engineering (2015), and 1 published the Journal Energies (2016).

Relevant background information to this work is given in introduction, followed by the objectives of the work in section 2. The experimental methods used are given in section 3. A simplified description of the heat transfer model used for analysis of some of the results in this work is presented in section 4, followed by the results and discussion in section 5. Conclusions and recommendations for future work are given in section 6.

The results presented and discussed in this dissertation are based on the papers mentioned above. These are listed below with Roman numerals according to the order of the works. Further referencing of the papers in this dissertation is given according to the numbering in this listing. The full papers are also attached in the appendix of this dissertation.

Paper I, presents the effect of methane hydrate concentration on the heat transfer through a hydrate-water slurry, without stirring. It also demonstrates an intuitive approach that can be used for heat transfer studies on gas hydrates.

Paper II, presents a study on the effect of parameters such as Temperature, Water content, Stirring rate, and Reactor size on gas hydrate growth kinetics.

Paper III, presents a study on estimating gas hydrate growth based on heat transfer. It highlights important factors related to modeling hydrate growth from heat transfer.

Paper IV, the effect of hydrate content on heat transfer through hydrate-water slurry has been extended from the study with methane hydrate in paper I, using Tetrahydrofuran (THF) and Ethylene oxide (EO) hydrate which offered better control of the hydrate content in the cell.

Paper V, is a study on the effect of parameters such as Temperature, Water content, Stirring rate, and Reactor scale-up on gas hydrate growth rate extended from paper II, with the growth rates normalized by the water content, and applied to the design of rapid hydrate formation systems.

Paper VI, is a review on the intermolecular interactions that govern clathrate hydrate related processes.

Acknowledgements

First and foremost I thank Jehovah God, the almighty for supporting me through my entire life, providing me this opportunity and granting me the ability to proceed successfully.

I would like to extend my profound gratitude to Dr. Thor Martin Svartås for excellent supervision during my PhD program and for providing interesting comments, ideas and encouragement. I appreciate all advantages that I have received from him. I also express my deepest gratitude to my Co supervisor Dr. Runar Bøe for his support and contributions during my PhD.

My deepest appreciation to all the students who have worked with me in the lab during their Bachelors and Masters projects, at various points in time performing experiments, some of which have been used in my PhD research.

I would like to thank all the technicians at the department of Petroleum Engineering, especially Sivert Drangeid and Svein Myhren, for all the time they dedicated to making sure my set-up was up and running. As well as Kim Andre Vorland, Ola Ketil Siqveland, and for their technical support. Also Inger Johanne Munthe-Kaas Olsen for her assistance in getting the chemicals used in this work.

I would like to express my best appreciation to the University of Stavanger and its staff. I would like to thank Kathrine Molde for her kindness and help during my PhD. My office mates Mahmoud Khalifeh and Ivan Dario P. Torrijos, for the understanding and cooperation. Thanks to Adekunle Peter Orimolade and Mesfin A. Belayneh for our insightful discussions and your

practical support. And all my colleagues at the Department of Petroleum Engineering, University of Stavanger for their support.

I express my sincere gratitude to my friends in Stavanger and abroad for their motivation and encouragements.

Finally, many thanks to my family for all their support and encouragement throughout my PhD. I am very grateful for my mother Mrs. Edith Nimighayefa Ponomogha, and my Father Mr. Tariyemienyo Remi Meindinyo, and my siblings for their loving support through prayer and words of encouragement, I would not be who I am today without all you support and care.

Summary

Gas hydrate thermodynamics and phase equilibria is already well established. However, some knowledge gaps still need to be filled in gas hydrate growth kinetics, in relation to new gas hydrate based technologies in gas separation and storage; as well as in the modeling of gas hydrate growth from the mechanisms of intrinsic kinetics, mass transfer, and heat transfer. Our findings from this work contribute valuable insights to the ongoing discussion on gas hydrate growth kinetics.

New technologies in gas separation and storage require fast and efficient gas hydrate formation rates. In line with this, we have investigated the effect of parameters that may be optimized to give rapid gas hydrate growth rates, such as; temperature, water content, stirring rate, and reactor size on gas hydrate growth kinetics. This was carried out in two studies, in the first one, the growth rate was estimated directly from gas consumption rates in normal milliliters per minute [NmL/min]; while the second study was an extension of the first with the growth rate normalized by the water content (volume of water) in the cell. In line with this investigation, we have employed the correlation for the average bubble diameter from literature, based on isotropic turbulence theory for estimating the average bubble size; for analysis of the dispersion parameters of the system. The results from these studies reveal the following:

1. For the temperature: increased subcooling increases gas hydrate growth rates. Increased subcooling in this case gives a direct reflection of the effect of increased driving force.
2. For the water: increased water content gave poorer gas-liquid dispersion and thus slower gas hydrate growth rates.
3. For stirring: increased stirring increased the growth rate up to a threshold stirring rate beyond which further increase in the stirring rate

did not increase the gas hydrate growth rate. This was linked to negligible heat and mass transfer effects beyond the threshold stirring rate.

4. For reactor size (scale-up with geometric similarity): though more absolute volumes of gas hydrates was formed with increased reactor size, which is due to the increased volumes of reacting components, the growth rate per unit volume of water in the reactor decreased.

Furthermore, analyzing the effect of increased stirring in terms of power input per unit volume (P/V), increased power input per unit volume did not improve the gas-liquid dispersion parameters beyond the threshold stirring rate. With scale-up of reactor size, the results show that even at similar P/V and gas-liquid dispersion parameters, gas hydrate growth rate decreased.

In addition we have performed studies on the effect of hydrate content on heat transfer using methane hydrate, Tetrahydrofuran (THF) and Ethylene oxide (EO) hydrates. The measurements from the heat transfer experiments were analyzed using a simple heat transfer model. These studies revealed important insights on hydrate plug deposition behavior on the reactor wall, as well as heat transfer through the hydrate slurry with increasing hydrate content. A solid hydrate mass formed at 40 – 60% hydrate content. Also, the heat transfer coefficient decreased with increasing hydrate content, but remained constant once a solid hydrate mass formed. The heat transfer coefficient would change as hydrate growth progresses. Finally methane hydrate growth was modeled based on heat transfer. The findings from this study confirmed the transient nature of the heat transfer coefficient during hydrate growth and that hydrate growth can be modeled based on heat transfer if the transient nature of the heat transfer coefficient is taken into account.

List of papers

I. **R.-E. Meindinyo, T.**, T.M. Svartaas, and R. Bøe. "*Heat Transfer During Hydrate Formation - an Investigation on the Effect of Hydrate Content on the Heat Transfer Coefficient of Gas Hydrate Slurry*". in Proceedings of the 8th International Conference on Gas Hydrates (ICGH8-2014), Beijing, China, 28 July - 1 August, 2014.

II. **R.-E. Meindinyo, T.** and T.M. Svartaas. "*A Parametric Study of Hydrate Growth Behaviour*". in Proceedings of the 8th International Conference on Gas Hydrates (ICGH8-2014), Beijing, China, 28 July - 1 August, 2014.

III. **R.-E. Meindinyo, T.**, T.M. Svartaas, T.N. Nordbø, and R. Bøe, *Gas hydrate growth estimation based on heat transfer. Energy & Fuels*, 2015, 29.2: 587-594.

IV. **R.-E. Meindinyo, T.**, T.M. Svartaas, S. Bru, and R. Bøe. *"Experimental Study on the Effect of Gas Hydrate Content on Heat Transfer."* ASME 2015 34th International Conference on Ocean, Offshore and Arctic Engineering. American Society of Mechanical Engineers, 2015.

V. **R.-E. Meindinyo, T.** and T.M. Svartaas, "Gas Hydrate Growth Kinetics: A Parametric Study." *Energies* 9.12 (2016): 1021.

Additional works

VI. **R.-E. Meindinyo, T.**, T.M. Svartaas, *"Intermolecular Forces in Clathrate hydrate related processes."* ASME 2015 34th International Conference on Ocean, Offshore and Arctic Engineering. American Society of Mechanical Engineers, 2015.

Nomenclature

A	kinetic parameter in equation for nucleation rate
$A_{(g\text{-}l)}$	gas-liquid interfacial area, (m^2)
A_I	internal heat transfer surface area of the reactor, (m^2)
A_p	surface area of hydrate particle, (m^2)
A_s	crystal surface area, (m^2)
B'	thermodynamic parameter for hydrate nucleation, (K^3)
B^*	birth rate of hydrate crystals, (s^{-1})
C_b	solute concentration in the bulk phase, (mole/m^3)
C_{eq}	solute concentration at the crystal surface, (mole/m^3)
C_{int}	solute concentration at the gas-liquid interface, (mole/m^3)
c	numerical shape factor
c_p	constant pressure specific heat capacity, (J/kg K)
$c_{p,g}$	constant pressure specific heat capacity of gas phase, (J/mole K)
$c_{p,H}$	constant pressure specific heat capacity of hydrate phase, (J/kg K)
$c_{p,w}$	constant pressure specific heat capacity of water phase, (J/kg K)
D^*	death rate of hydrate crystals, (s^{-1})
f_i^b	fugacity of bulk phase, (MPa)
f_i^{eq}	equilibrium fugacity, (MPa)
G	linear growth rate of hydrate, (m/s)
ΔG	excess Gibbs free energy, (J)
ΔG_{crit}	excess Gibbs free energy barrier for hydrate nucleation, (J)
ΔG_S	surface excess Gibbs free energy, (J)
ΔG_V	volume excess Gibbs free energy, (J)
Δg_V	Gibbs free energy per unit volume, (J/m^3)
h_I	Internal heat transfer coefficient through hydrate slurry to cell wall, (W/m^2 K)
ΔH_{gen}	enthalpy of hydrate generation, (J/mole)
Δh_e	experimentally accessible enthalpy of hydrate dissociation at the equilibrium temperature, (J)
J	nucleation rate, (m^{-3} s^{-1})
K'	overall crystal growth rate constant, (mole/m^2 MPa s)
K^*	overall hydrate growth rate constant, (mole/m^2 MPa s)
k	Boltzmann constant, (J/K)
k_d	mass transfer (diffusion) coefficient of solute across solution-crystal interface, (mole/m^2 MPa s)
k_L	liquid phase gas-liquid mass transfer coefficient, (mole/s)

k_r	reaction coefficient at crystal surface, (mole/m^2 MPa s)
m	mass, (kg)
m_H	mass of hydrate, (kg)
m_w	mass of water, (kg)
N_g	moles of gas inside reactor, (mole)
N_{Re}	Reynolds number
n	moles of gas consumed for hydrate formation, (mole)
$\dot{q}_R$	heat generation rate from hydrate formation, (J/s)
R_y	global growth rate of gas hydrate, (mole/m^3 s)
r	radius, (m) (also radius of cell / distance from cell center in chap 4)
r_c	critical nuclei radius for hydrate nucleation, (m)
ΔS_e	entropy of hydrate dissociation at the equilibrium temperature, (J/K)
T	temperature, (K)
T_b	temperature in the bulk phase, (K)
T_e	equilibrium temperature of hydrate formation, (K)
T_{eq}	temperature at the crystal surface, (K)
T_{int}	temperature at the gas-liquid interface, (K)
T_I	reactor internal temperature, (K)
T_w	reactor wall temperature, (K)
ΔT	subcooling, (K)
t	time, (s)
V_n	molar volume of gas, (NmL/mole)
v_h	volume of hydrate building unit, (m^3)
α	thermal conductivity, (W/m K)
θ	angle of wetting between hydrate crystal and a contacting surface, (°)
μ_n	n-th moment of crystal particle size distribution, (m^n/m^3)
μ_n^0	initial n-th moment of crystal particle size distribution
σ	interfacial tension, (J/m^2)
ϕ_p	crystal particle size distribution, (m^{-4})

Table of contents

1. Introduction

1.1. Gas hydrates

Gas hydrates are ice-like crystalline compounds composed of water and small gas molecules. They usually form under conditions of high pressure and low enough temperatures. The temperatures at which gas hydrates form are usually higher than the ice point of water, making it a unique phenomenon. Gas hydrate formation is characterized by microscopic and macroscopic processes that have made them a huge subject of scientific and engineering curiosity. Gas hydrate formation is governed by some unique intermolecular interactions [1]. When hydrates form, water molecules encage gas molecules situated in their vicinity through a process called hydrophobic hydration [1]. Here the water molecules are called “hosts”, while the encaged gas molecules are called “guests”. The hydrophobic hydration process is primarily driven by the hydrogen bonding tendency of the water molecules. In an effort not to lose any hydrogen bonding due to the presence of non-polar gas molecules, the water molecules reorder so that they form a cage-like structure around the gas molecule. The size and shape of the resulting cage depends on the size of the gas molecule being encaged (**Figure 1**). [1, 2]

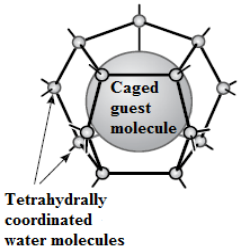

Figure 1. Water molecules form a "cage" around a "guest" gas molecule via hydrophobic hydration (Image adapted from Israelachvili (2011) [1]).

There are various cages or “cavities”, which combine in different ratios to form larger polyhedral gas hydrate structures (**Figure 2** and **Figure 3**). The most common gas hydrate structures are structure I (sI), structure II (sII), and structure H (sH). sI hydrate consists of 2 pentagonal dodecahedron (5^{12}) small cavities, and 6 tetrakaidecahedron ($5^{12}6^2$) large cavities; sII hydrate consists of 16 pentagonal dodecahedron (5^{12}) small cavities, and 8 hexakaidecahedron ($5^{12}6^4$) large cavities; and sH hydrate consists of 3 pentagonal dodecahedron (5^{12}) small cavities, 2 irregular dodecahedron ($4^3 5^6 6^3$) medium cavities, and 1 icosahedron ($5^{12}6^8$) large cavity. The cavities have a water molecule at each of their vertices. For example the pentagonal dodecahedron cavity which has 20 vertices has a total of 20 water molecules, the tetrakaidecahedron has 24 water molecules, the hexakaidecahedron has 28 water molecules, the irregular dodecahedron has 20 water molecules, and the icosahedron has 36 water molecules. The unit cell of structures sI, sII, and sH hydrates have an average of 46, 136, and 34 water molecules respectively. The cavity structure and size may have an effect on the properties of the different hydrate structure types, though this would be mainly an effect of the organization and orientation of the water molecules, which form the bulk of the hydrate volume (ca. 85%). [2] (pp. 53 – 71).

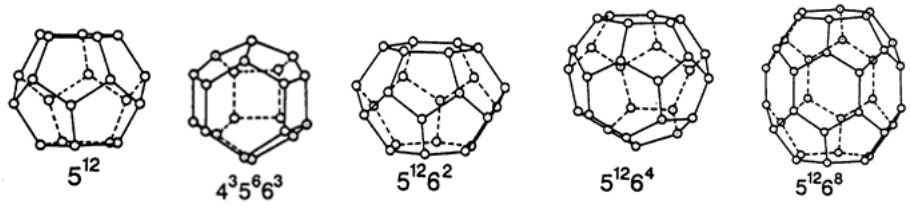

Figure 2. Gas hydrate cavities (pentagonal dodecahedron, irregular dodecahedron, tetrakaidecahedron, hexakaidecahedron, and icosahedron).

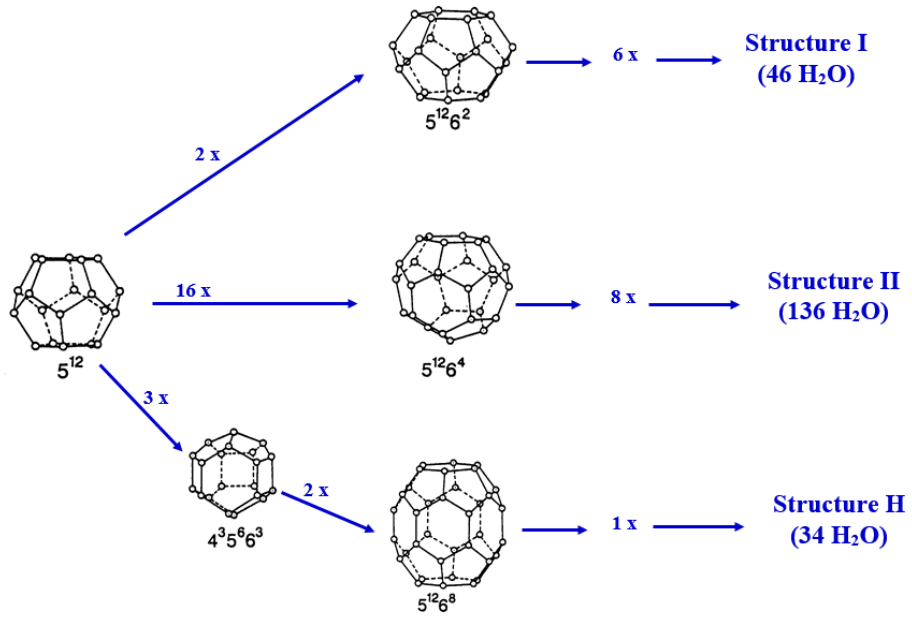

Figure 3. Common Gas hydrate Structures.

Smaller hydrate guest molecules would preferentially stabilize the smaller cavities, while larger guest molecules would stabilize the larger cavities. Each cavity can be stabilized by one guest molecule or more, but the cavity stability depends on the guest/cavity size ratio. Methane, ethylene oxide (EO), and tetrahydrofuran (THF), were used as hydrate formers in this work. Both methane and EO form sI hydrate, while THF forms sII hydrate. In methane hydrate, one methane molecule occupies each of the small and large cavities respectively, with a guest/cavity size ratio of 0.86 and 0.74 respectively. The lattice parameter also gives an indication of the average guest/cavity filling ratio of a given hydrate structure, and the relative stability of the hydrate formed by different guest molecules. For a given hydrate structure, the hydrate former with a larger lattice parameter forms a more stable hydrate. Thus, EO hydrate which has a lattice parameter of 12.1Å has an equilibrium temperature of about 11.1°C

at atmospheric pressure, and methane hydrate which has a lattice parameter of 11.981Å requires a pressure of 81.6 bars to form hydrate at the same temperature. Though, one must not neglect the role that the solubility of EO in water plays in reducing its hydrate equilibrium pressure. The cavity size changes slightly depending on the guest molecule size and the hydrate structure formed. The lattice parameters are also a function of temperature, pressure, and guest molecule size.

At normal pressures, only one guest molecule would occupy each hydrate cavity. i.e., the ideal guest to water combining ratio for SI hydrate is 1:5.75, and for SII hydrate is 3:17. However, there is never a 1:1 filling ratio for all cavities in a given hydrate structure. Thus, the result is a non-stoichiometric combining ratio between the guest molecules and the water molecules. There is usually an excess of water molecules available compared with the ideal guest to water combining ratio, as some of the cavities remain unoccupied when hydrates form. Therefore, it is common to assume a combining ration of 1 guest : 6 water molecules for sI hydrate. The cavity filling would increase with increasing pressure, and at very high pressures cavity occupancy by more than one guest molecule has been documented.

The cavity stability also determines what hydrate structure a given hydrate former would preferentially form. For example, methane and CO_2 both have a guest/cavity size ratio for the small and large cavities of 0.86 and 0.74, and 1 and 0.834 respectively for sI hydrate; 0.868 and 0.655, and 1.02 and 0.769 respectively for sII hydrate. This implies they both have more stable cavities when they form SI hydrate, and will thus preferentially form simple hydrates of sI. Judging by the same principle, the simple sI hydrate of CO_2 will be more stable than that of methane. Therefore, a system containing methane hydrate can be converted to CO_2 hydrate if exposed to CO_2. The much higher solubility of CO_2 in water also aids this process, because CO_2 requires a lower hydrate

stability pressure than methane. Some of these principles of hydrate relative stability have been capitalized on in the emerging fields of hydrate based new technologies.

Gas hydrates are a subject of interest in various fields: flow assurance, drilling and well operations, exploration geology, energy resource, storage and transport medium for natural gas, CO_2 capture, desalination of water, environmental pollution, and other new technological applications [2] (pp. 537 – 679), [3-17]. There is a lot of ongoing research related to the aforementioned subject areas, more of which is presented in section 1.3. There is no doubt in the immense benefits associated with a clearer understanding of the hydrate related issues on the different levels mentioned. The key to such understanding lies in a good knowledge base on the microscopic and macroscopic interactions which define gas hydrate formation kinetics.

1.2. How hydrates form

Certain conditions are necessary, for hydrates to form. These are: presence of water, hydrate forming guest molecules, a high enough pressure, and low enough temperature. It is striking that gas hydrates readily form above the ice point of water, a factor that made the phenomenon seem unusual when it was first encountered [2] (p. 1,2). The presence of these basic criteria for hydrate formation does not serve as fact of hydrate formation. Hydrate formation is influenced by a dynamics of several other factors, which we will touch on as we progress. Hydrate formation is a crystallization process that involves two distinct stages; nucleation, followed by crystal growth.

1.2.1. Gas hydrate nucleation

When hydrate forming gas molecules dissolve in water, the water molecules driven by their tendency to keep their intra-molecular hydrogen bonding, begin

to organize around the gas molecules. This re-organization of water molecules around gas molecules creates small gas-water clusters which form the sites for nucleation to commence. The re-organization to create a new surface, reduces the system entropy leading to a positive surface excess Gibbs free energy ($\Delta G_{s)}$ as shown in **Figure 4**. The released enthalpy from the mass of the growing cluster contributes with a negative volume excess Gibbs free energy (ΔG_v). For spontaneous hydrate growth to commence, the clusters must aggregate to attain a critical cluster size.

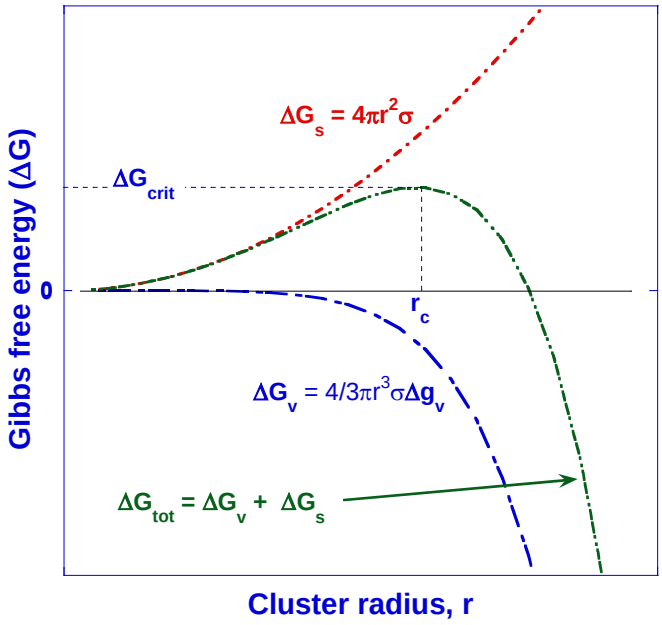

Figure 4. Illustration of Energy perspective to gas hydrate nucleation.

Before clusters attain the critical size they may shrink or grow, this leads to a metastable period till the critical cluster size is attained, after which spontaneous crystal growth commences [2, 18]. The metastability during

nucleation can be viewed from an energetic perspective. In the course of formation of solid hydrate particles from solution, the excess Gibbs free energy between a small solid particle of solute and the solute in solution is given as ΔG. Here, ΔG equals the sum of the surface excess Gibbs free energy ΔG_S and the volume excess Gibbs free energy ΔG_V, given as

$$\Delta G = \Delta G_S + \Delta G_V = 4\pi r^2\sigma + \frac{4}{3}\pi r^3 \Delta g_v \qquad (1)$$

ΔG_S is associated with solute molecules becoming part of the surface of the crystal nuclei and is a positive value (due to increasing order and decreasing system entropy), ΔG_v is associated with the solute molecules becoming part of the bulk of the crystal nuclei (carrying released energy of formation) and is represented by a negative value (enthalpy), Δg_v is the free energy change per unit volume, and σ is the surface tension of the crystal-liquid interface. The surface and volume contributions lead to a maximum excess Gibbs free energy value, ΔG_{crit} at the critical radius r_c. Before attaining the critical radius, the energy costs for increased nuclei size is high, the competition between surface and volume energy thus keeps the nuclei in a shrink-grow "jigsaw" situation, causing metastability. [2, 18-20] At a critical cluster size [18] the surface excess free energy change balances the volume excess free energy change, the total excess free energy gradient, $\delta(\Delta G)/\delta r$, becomes zero and the formed nuclei become stable and growth may commence.

The nucleation concept discussed above and the expression for the critical Gibbs free energy of nucleation obtained is for a case with complete non-wetting of the substrate, and is called homogenous nucleation (HON). Homogenous nucleation would only occur in the bulk volume of an ultra-pure system free of any micro particles or surfaces. It is therefore rarely encountered in reality. The more commonly encountered case of nucleation is heterogeneous nucleation (HEN). The presence of additional surface area from micro particles,

gas-liquid interfaces, or container walls, reduces the critical Gibbs free energy required for heterogeneous nucleation, $\Delta G'_{crit}$, which is given as

$$\Delta G'_{crit} = \phi \cdot \Delta G_{crit} \quad (2)$$

where ϕ is a function of the angle of wetting, θ, between the hydrate crystal and the surface it is related to, given as

$$\phi = [(2 + cos\theta)(1 - cos\theta)^2]/4 \quad (3)$$

where the angle $\theta = 180°$ for a completely non-wetting surface, in which case we have homogenous nucleation, and $\Delta G'_{crit} = \Delta G_{crit}$. $\theta = 180°$ for a completely wetting surface.

Nucleation rate, (J), is the rate at which hydrate nuclei aggregate to achieve the critical cluster size. J has a unit of [m^{-3} s^{-1}]. Kashchiev and Firoozabadi [21] proposed an expression for the nucleation rate at constant pressure, from classical nucleation theory as

$$J = A \cdot exp(\frac{\Delta S_e \Delta T}{kT})(-\frac{B'}{T\Delta T^2}) \quad (4)$$

where A, is a kinetic parameter that depends on the type of nucleation; HON or HEN, and the type of surface in contact with the hydrate crystal. ΔS_e (J/K), is the entropy (per hydrate building unit) of hydrate dissociation at the equilibrium temperature, T_e (K). ΔS_e can be estimated from the relation, $\Delta S_e = \Delta h_e/T_e$; where Δh_e (J), is experimentally accessible enthalpy (per hydrate building unit) of hydrate dissociation at the equilibrium temperature T_e. ΔT (K) is the subcooling, k (1.3805 $\times 10^{-23}$ J/K), is the Boltzmann constant, T (K), is the system temperature, and B' (K^3), is the thermodynamic parameter given as

$$B' = 4c^3 v_h^2 \sigma^3 / 27k\Delta S_e^2 \quad (5)$$

where c is the numerical shape factor, v_h (m^3) is the volume of hydrate building unit, and σ (J/m^2) is the specific surface energy or surface tension of the hydrate per unit solution interface.

Mullin [18] has earlier proposed a general expression for the nucleation rate of crystallization processes as

$$J = A \cdot exp(-\frac{\Delta G_{crit}}{kT}) \quad (6)$$

Equating equ (4) and (6), we get an expression for the critical Gibbs free energy change of phase transition as

$$\Delta G_{crit} = \frac{4c^3 v_h^2 \sigma^3 (\Delta T) T_e}{27 k \Delta h_e} \quad (7)$$

Equ (7) shows that at constant pressure, the Gibbs free energy change of phase transformation is a linear function of the subcooling, and is inversely correlated with the enthalpy. Thus, as the Gibbs energy barrier for phase transition is reduced, the amount of heat released during hydrate growth increases.

The metastability associated with nucleation makes the process stochastic. Meaning that for a given set of conditions, the time from which a hydrate forming system falls into the hydrate formation region to the time of visible hydrate formation will vary widely [22] (p. 2), [23-26]. Thus a statistical approach has been employed in nucleation studies, requiring a repetition of several experimental runs at the same conditions [22, 27-33]. This statistical approach involves assigning probabilities of nucleation to different induction time measurements. The probability values are equal to the frequency of duration of each measurement, from a total set of N experiments. The longest induction time having the highest probability value, and the shortest induction time having the lowest probability value. These statistical methods have been thoroughly addressed in a number of studies [27, 32].

The induction time for crystallization process is defined as is the amount of time between the achievement of constant supersaturation and the detection of crystals [18, 31]. As observed in this work, for a constant pressure process, this would be the duration from the start of stirring, when the system attains an isothermal state till a temperature spike is observed (**Figure 5**).

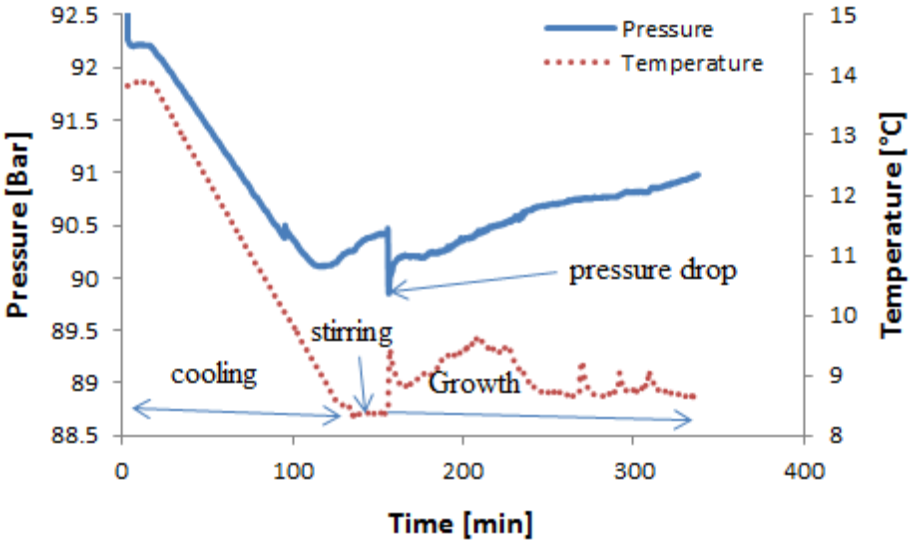

Figure 5. A constant pressure hydrate formation experiment in a 191.4 mL stirred reactor. The figure shows changes in pressure and temperature within the cell during cooling, stirring, and hydrate growth. The time from start of stirring to the spike in temperature is equal to the experimentally measured induction time.

As seen from **Figure 5**, once the system is cooled to the desired experimental temperature, the temperature remains constant, indicating a constant supersaturation. At this point, the system is still in the metastable stage of the nucleation process. Once the critical nucleus is formed, a clear sign of hydrate growth is seen with a rapid temperature rise due to release of the enthalpy of hydrate formation. The slight fluctuations in the system pressure during this period ($\pm 0.5\ bars$)would have negligible effect on the system saturation.

Rapid hydrate formation requires reducing or if possible eliminating the induction time for hydrate crystallization.

The start of hydrate growth does not mean the end of nucleation, rather secondary nucleation occurs [2, 18], which also serves to feed the already growing crystal. The presence of a growing crystal makes further nucleation much easier, due to the energetic advantages provided by the additional surface area from the growing crystal surface. This mechanism of secondary nucleation has been employed in “cold flow technology” to quicken water conversion to hydrate [34-36]. The memory effect phenomenon which suggests that hydrates retain a memory of their structures when melted at moderate temperatures, and thus would form more readily from water with hydrate history than from fresh water with no hydrate history; is in part explained by an hypothesis similar to the mechanism of secondary nucleation. This hypotheses on memory effect has been suggested in works by Makogon [37], Lederhos et al. [38], Takeya et al. [39], Ohmura et al. [28], Buchanan et al. [40], and others [23, 41-44]. However, Wilson and Heymet in their work with THF/water mixtures [45], have argued that they found no evidence of a memory effect. The memory effect technic is also used by some gas hydrate researchers to make the nucleation process less stochastic, to provide a good baseline for testing of chemicals for inhibition of gas hydrate nucleation and growth [38].

The mechanism of secondary nucleation and memory effect have important implications for the oil and gas industry both in flow assurance and industrial scale production of gas hydrates. For example, upon dissociation of a hydrate plug in a pipeline, the residual water phase must be properly handled (removed, or heated to a temperature that ensures that any persistent crystallites or structure is eliminated), otherwise, rapid reformation of hydrate plug can occur [2]. Conversely, the memory effect phenomenon and secondary nucleation can

be used to reduce or eliminate the nucleation time for processes where rapid hydrate formation is desired.

1.2.2. Gas hydrate growth

Gas hydrate growth is the next stage in the hydrate formation process, once critical nuclei are formed. The conceptual picture of the growth of gas hydrates at the molecular level, shows that hydrate growth may consist of several steps, driven by intermolecular interaction forces [2] (Paper VI). Gas hydrate growth has been modeled based on a boundary layer theory that includes film layers between the gas – liquid-bulk and liquid-bulk – hydrate-crystal phases. We have adopted the schematic picture by Mork [46], which shows that there will be a concentration and temperature gradient across the gas – liquid-bulk , and liquid-bulk – hydrate-crystal phases (**Figure 6**).

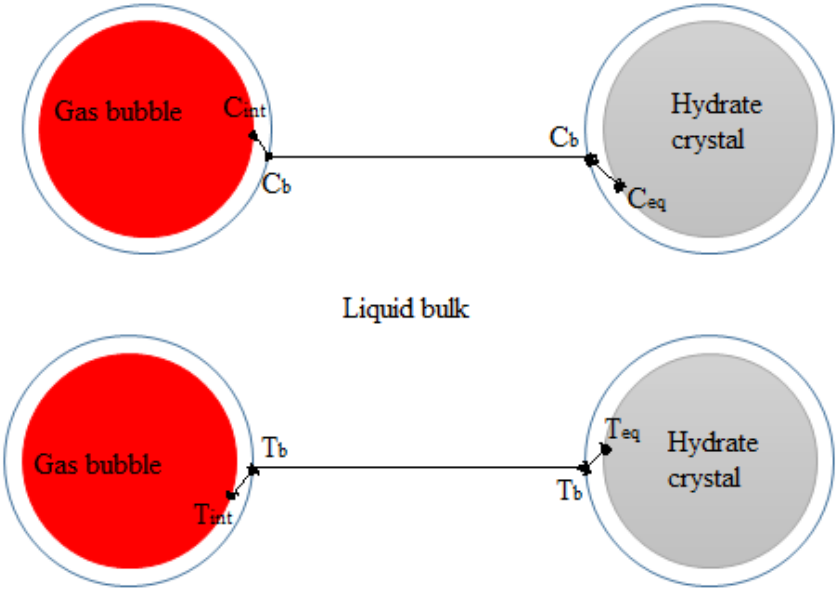

Figure 6. Schematic illustration of gas – liquid and crystal – solution interfaces for mass transfer of gas through bulk phase to the crystal surface in a hydrate forming system (concept has been adopted from Mork (2002) [46]).

At the gas – liquid-bulk interface, the gas and liquid phases are at equilibrium at the system temperature and pressure. There is a drop concentration of the gas from the interface across the liquid side film layer to the liquid bulk from C_{int} to C_b. Also, the temperature rises across the liquid side film layer due to gas dissolution from T_{int} to T_b. At the crystal end of the liquid-bulk – hydrate-crystal interface the gas is at the hydrate equilibrium conditions. Concentration of the gas drops to its value at the hydrate equilibrium conditions, C_{eq}, and the temperature increases to the hydrate equilibrium temperature, T_{eq}. The concentration and temperature gradients serve as driving forces for the transport of gas. Accordingly, models and correlations for gas hydrate growth have been based on the rate of gas transport across gas-liquid interface, the liquid-crystal interface and the inclusion rate of gas at the crystal surface, as

well as the heat transport from the crystal surface to the bulk phase and from the bulk phase.

The following part of the discussion is mainly based on excerpts from Sloan and Koh [2], Mork [47], and Jensen [48].

Describing gas hydrate growth based on intrinsic kinetics

Noyes and Whitney [49] originally proposed a model for crystal growth rate based on diffusion from the bulk phase to the crystal equilibrium interface as the controlling mechanism

$$dm/dt = k_d A_s(C_b - C_{eq}) \quad (8)$$

where A is the crystal surface area, and k_d is the mass transfer coefficient. Berthoud [50] and Valeton [51] later proposed a modification to this concept suggesting that the crystal growth consisted of two steps, first diffusion to the crystal equilibrium interface, followed by reaction at the interface. Thus the model was modified to

$$dm/dt = K' A_s(C_b - C_{eq}) \quad (9)$$

where K' is the overall transfer coefficient, which consists of the coefficients for diffusion k_d, and reaction k_r, and is given as

$$K' = \frac{1}{k_d} + \frac{1}{k_r} \quad (10)$$

Building on these classical theories, Englezos et al. [52] proposed an intrinsic kinetic model of gas hydrate growth based on the rate of transport of gas, (dn/dt), from the bulk phase to the crystal surface, and the inclusion of the gas at the crystal surface into the hydrate structure.

The Englezos et al. [52] model defines the growth rate per hydrate particle as

$$(dn_i/dt)_p = K^* A_p\left(f_i^b - f_i^{eq}\right) \quad (11)$$

where K^* is the hydrate growth rate constant incorporating combined the mass transfer coefficient of the gas across the liquid-crystal interface and the reaction coefficient at the crystal surface. A_P is the surface area of each hydrate particle. $(f_i^b - f_i^{eq})$ represents the overall driven force, given by the difference in the gas fugacity in the liquid-bulk and at the hydrate equilibrium conditions. This model has been improved upon in subsequent works to address some accompanying limitations and inconsistencies [53-57]. To formulate the global reaction rate, the rate per particle is integrated for all growing particles. The total surface area of all growing particles is thus a function of a particle size distribution, and can be presented in terms of the second moment of the particle size distribution as

$$A_p(t) = 4\pi\mu_2 \quad (12)$$

giving an expression for the global growth rate as

$$R_y(t) = 4\pi K^* \mu_2\left(f^b - f^{eq}\right) \quad (13)$$

where μ_2 is the second moment of the particle size distribution, given as

$$\mu_2 = \int_0^\infty r^2 \phi_p(r,t)dr \quad (14)$$

A population balance is required to estimate μ_2 as a function of time, given by

$$\frac{d\phi_p}{dt} + G\frac{d(\phi_p)}{dr} = B^* - D^* \quad (15)$$

Φ_p (m) is the particle size distribution, t (s) is time, G (m/s) is the linear growth rate, which is independent of the size of the growing crystal, r (m) is the particle radius, B* and D* are the birth and death rates, i.e. the number of particles that grow into and shrink out of the size range of the particle size distribution due to primary nucleation, secondary nucleation, agglomeration, and breakage. The

particle size distribution can be analyzed via in-situ methods like Focused Beam Reflectance Measurement (FBRM). Clark and Bishnoi [58] determined via FBRM that the number of particles remain constant once growth commences. That means the term on the right hand side of equ (15) equals zero, and the population balance becomes

$$\frac{d\phi_p}{dt} + G\frac{d(\phi_p)}{dr} = 0 \tag{16}$$

The population balance can now be solved for the second moment of particle distribution to get

$$\mu_2 = \mu_0^0 G^2 t^2 + \mu_1^0 G t + \mu_2^0 \tag{17}$$

where $\mu_0^0, \mu_1^0, \mu_2^0$, are the initial number, size, and surface area of particles, respectively.

Thus the total surface area of the growing particles becomes

$$A_p(t) = 4\pi(\mu_0^0 G^2 t^2 + \mu_1^0 G t + \mu_2^0) \tag{18}$$

Showing that the particle surface area is a quadratic function of time, and thus a crystal growth process that is controlled by intrinsic kinetics is expected to be non-linear.

Describing gas hydrate growth based on mass transfer across the gas-liquid interface

Skovborg and Rasmussen [59] tested the model by Englezos et al. over a long rang of time and discovered that the model predicted an increasing growth rate with time, contrary to the measurements from experiments which showed a decreasing growth rate with time. Skoveborg and Rasmussen thus argued that the decrease in measured rate with time is because the gas consumption rate does not depend on the total surface area of the growing particles, rather it is controlled by the transport of gas across the gas – liquid interface instead of integration into the crystal structure. They proposed a model of hydrate growth

based on mass transfer of gas across the gas – liquid interface, where the growth rate is presented as

$$dn/dt = k_L A_{(g-l)} c_{wo} (x_{int} - x_b) \quad (19)$$

where k_L is the liquid-side mass transfer coefficient, $A_{(g-l)}$ is the gas-liquid interfacial area, c_{wo} is the initial concentration of water, x_{int} and x_b are the interfacial and bulk mole fractions of the gas. Sloan and Koh's review of the Skovborg and Rasmussen model indicates that the model has several accompanying limitations [2].

It is reasonable to consider the transport of gas from the gas phase into the bulk, as the concentration of gas in the bulk phase is a direct function of the gas transport/dissolution rate. In turn, the transport/dissolution rate is a function of the gas-liquid volumetric mass transfer coefficient, k_La, which has a complex relationship with other parameters [60] (paper V).

Describing gas hydrate growth based on heat transfer

Some of the heat transfer based models of gas hydrate growth include those by Uchida et al. [61], Mori [62], Freer et al. [63], and Mochizuki and Mori [64]. Uchida et al.'s model was based on the following assumptions: 1) hydrate crystals form only at the front of a growing hydrate film, 2) one-dimensional conduction of heat from the film front to the water and guest fluids, 3) the heat removed from the front is balanced by heat generated from hydrate formation. Mori [62] proposed a lateral hydrate film growth model at the gas-water interface, with the assumption of convective heat transfer. Freer et al. [63] also proposed one-dimensional conductive heat transfer model for methane hydrate film growth at the methane-water interface. Mochizuki and Mori [64] later reviewed the preceding three models, and proposed a transient 2-dimensional conductive heat transfer model for the hydrate film growth. In this model, the

linear growth rate of the hydrate film along the water/guest interface, v_f is related to the lateral increase in the position of the hydrate film front

$$v_f = dx_h/dt$$

The heat balance at the film front is then given by

$$\rho_h \delta \Delta h_H v_f = \int_0^{\delta} \left(\lambda_h \frac{\partial T}{\partial x} \Big|_{x=x_{h-}} - \lambda_w \frac{\partial T}{\partial x} \Big|_{x=x_{h+}} \right) dy$$

where δ is the hydrate film thickness; $\lambda_h \frac{\partial T}{\partial x} \Big|_{x=x_{h-}} and\ \lambda_w \frac{\partial T}{\partial x} \Big|_{x=x_{h+}}$ are the hydrate-side and water-side temperature gradients respectively, at x = xh; x is the lateral position of the hydrate film front; Δh_H is the heat of hydrate formation per unit mass of hydrate; λ_h and λ_w are the thermal conductivity of hydrate and water respectively.

All the heat transfer models assume that rate of hydrate film growth is proportional to the rate of heat removal from the hydrate film. If the rate of heat removal from the growing hydrate film front is proportional to the lateral film growth rate, and a function of subcooling; then in stirred reactors where the heat absorbed from the hydrate film front may accumulated in the hydrate-water-guest mix, while some is removed from the reactor via cooling, we can relate the global macroscopic growth rate to the heat flux out of the system by establishing a heat balance.

It is worthy of note though that, one or more of the mechanisms described above may control hydrate growth, depending on the system in which gas hydrates are formed [2]. For example both heat and mass transfer will play significant roles in stirred systems and multiphase systems, while in systems with no heat or mass transfer restriction the hydrate growth rate is controlled by intrinsic kinetics [2, 19, 47, 65-68]. THF and Ethylene Oxide systems are good options to study gas hydrate intrinsic kinetics since both hydrate formers are soluble in water, and the solution can easily be made supersaturated throughout

the volume of the bulk [2, 69]. There have been several efforts put into modeling gas hydrate growth based on intrinsic kinetics [52, 58, 70], mass transfer [59], heat transfer [62, 71, 72], and more recently coupled mass and heat transfer or all three mechanisms in one model [65, 66].

Hydrate growth is a more predictable process; results for the same conditions are quite reproducible. Hydrate growth kinetics is affected by several parameters, most of which also affect the nucleation. Factors such as temperature, pressure, supersaturation, subcooling, and degree of agitation have been shown to affect hydrate growth [2, 41, 52, 73-75]. Understanding the effect of these parameters of gas hydrate formation is crucial to proper hydrate management and handling, as well as optimizing gas hydrate production processes.

Hydrate growth kinetic studies have been done using experimental methods that focus on the macroscopic growth process. Molecular dynamic studies have also provided better understanding on hydrate formation at a microscopic scale. [2] A common reactor set-up used for laboratory scale studies on gas hydrate growth kinetics is the stirred tank reactor either as a batched reactor, semi-batch reactor, or continuous reactor [2, 46, 52, 54, 55, 76-79]. These reactors provide a good modeling basis for the gas hydrate formation processes that occur in oil and gas networks, as well as for industrial scale production of gas hydrates.

1.3. Gas hydrate related issues

Although gas hydrate research started as a scientific curiosity on chlorine and inorganic gases, recent research on gas hydrates have been focused on providing solutions to different gas hydrate related issues. Gas hydrate issues cut across different disciplines, but are especially related to the petroleum/energy industry. They are a subject of interest as a nuisance, as a resource, or as potential for new technology.

1.3.1. As a nuisance

Gas hydrates first became of high interest to the oil and gas industry when Hammerschmidt discovered in the mid-1930s; that an ice-like substance plugged gas transmission lines, above the freezing point of water. This meant high economic losses, since plugged pipelines meant production had to be stopped (**Figure 7** – illustration of hydrate plug development). Hydrates will readily form if conditions are right for their formation, and are the most common flow assurance problem faced in the oil and gas industry [2-7, 80-82]. Thus much effort has been put into the remediation of hydrate plugs when they form, and prevention of hydrate formation; but in more recent times efforts are also being directed towards hydrate risk management.[5]

A better understanding of gas hydrate thermodynamics and kinetics have been crucial for successful handling of hydrates in flow assurance. Physical methods such electrical heating are being employed in subsea transmission lines to keep the temperature above hydrate formation conditions.[83-87] Also chemical methods such as the use of thermodynamic hydrate inhibitors (THIs), which shift the pressure-temperature conditions out of the hydrate region have aided with the prevention of hydrate formation, and plug remediation. But due to the high costs associated with the requirement for high dosages of THIs, recent efforts are being directed at the low dosage hydrate inhibitors (LDHIs), which are further divided into two groups; kinetic hydrate inhibitors (KHIs) and anti-agglomerates (AAs). Dosages of LDHIs required are less than 0.1 of THI dosages. LDHIs also offer a time dependent approach to gas hydrate management which is cost effective. [3, 88, 89]

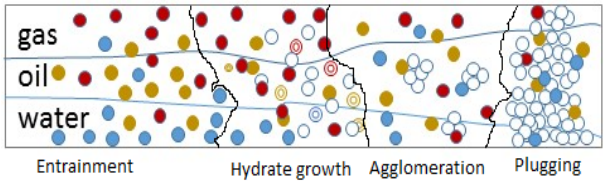

Figure 7. Illustration of hydrate plug development in a multiphase flowline, an adaptation of the figure by Zerpa et al. [7] taken from [20].

Gas hydrates may also cause well integrity issues during drilling operations, when present in reservoir sediments. This is due to disparity in mechanical and thermal properties of the hydrates from the reservoir rocks and the fluids saturating them, which may lead to hazards, when extracting conventional hydrocarbons [90-93].

Furthermore, there are huge amounts of methane hydrate deposits on the ocean floor around the globe as well as in permafrost regions of e.g. Siberia and onshore Canada. The dependence of methane hydrate stability on temperature means that with a rising sea water temperature, there exists a risk of dissociation of the methane hydrate deposits on the sea floor. Methane is a greenhouse gas, and its release to the atmosphere in this way will add to environmental concerns about global warming [94, 95].

1.3.2. As a resource

Huge amounts of methane gas are naturally stored in hydrate form around the permafrost regions and the ocean floor around the globe, most of which comes from biogenic and thermogenic sources, or the upward migration of methane gas which is converted to hydrate when the thermodynamic conditions allow for this [2, 8]. Estimates of methane gas reserves in hydrate form are believed to be 10 times more than all the conventional gas resources at present [96, 97]. Thus gas hydrates portend a very significant gas resource for the future.[9, 10,

98] This is especially important as the world moves towards a renewable energy future, gas which is cleaner than petroleum is considered a suitable standby energy. Producing the gas from these gas hydrate reserves may well fill this need. There is a lot of ongoing research into understanding the most reasonable means of exploiting this future energy source [99-104].

1.3.3. As potential technology

Findings from gas hydrate phase equilibria and formation kinetics have inspired research on gas hydrate based new technology in gas production, storage, transportation, and separation. Some gas hydrate formers such as CO_2 form more stable hydrates than methane at the same conditions, thus CO_2 gas can replace methane gas from methane hydrate deposits. In this way, unwanted CO_2 may be stored through sequestration in hydrate form while simultaneously producing methane gas for use as energy [105-108]. CO_2 may also be stored away in very dip aquifers in hydrate form, thus reducing the CO_2 signature in the atmosphere [106, 109-116]. Methane hydrate is stable at temperatures and pressures that provide safer conditions for the storage and transportation of gas, compared with LNG. Thus gas storage and transportation in hydrate form is being considered as a viable option to LNG [117, 118]. Also, scientists are looking into the possibility of exploiting the inclusion mechanisms of gas hydrate and the difference in stability of different hydrate formers in gas separation as a new technology [13-15, 119].

1.4. Motivation

With over a century of research on gas hydrates, a lot of progress has been made, and there is good knowledge base particularly in the thermodynamics of hydrate formation and gas hydrate phase equilibria. [2, 37] However, a number of gaps still need to be filled in our understanding of gas hydrate formation

kinetics. Challenges still exist in connection to how mechanisms such as intrinsic kinetics, mass transfer, and heat transfer, can be related to hydrate growth. It has been argued that heat and mass transfer may play a more significant role for gas hydrate growth, than intrinsic kinetics, in multi-phase systems. [2, 19] Gas hydrate formation is exothermic process and is associated with release of formation enthalpy. [3, 71] During experiments in high pressure cells this energy release results in a temperature increase which is balanced when the heat loss to the surrounding cooling cap equals the heat inflow from the continuous hydrate production. Then is it possible to model the hydrate growth kinetics through temperature measurements combined with heat transfer calculations? Part of this work has been on the possibilities to describe hydrate growth kinetics through temperature measurements and heat transfer in a hydrate forming system. We have chosen methane hydrate as model system since the hydrate formed is well defined and its formation enthalpy per mole of gas consumed is known from literature [120].

Secondly, new gas hydrate based technology in gas separation and storage, requires quick and efficient hydrate formation. There is a need for fundamental understanding on the key factors that will enable rapid and efficient production of gas hydrates.

To address these subjects, we have broken down the research goals in this work in the following chapter on titled “objectives”.

2. Objectives

The objective of this work has been to contribute to a better understanding on factors that affect gas hydrate growth kinetics with a focus on the two main areas which motivated this work: 1) Heat transfer as it relates gas hydrate growth kinetics, and 2) Consider parameters we can optimize to obtain rapid gas hydrate growth rates.

In doing this, different experimental methods, as well as a simple heat transfer model have been used to

- investigate the effect of hydrate content on heat transfer through hydrate slurry, under quiescent and stirred conditions.
- model hydrate growth based on heat transfer.
- investigate the effect of parameters such as temperature, stirring rate, water content (water-cut), and reactor size, on hydrate growth behavior.

Our findings and the results discussed in this thesis provide valuable understanding on the modeling of hydrate growth based on heat transfer, and the key factors to focus on when designing systems for rapid hydrate production.

3. Experiments

In this section, a description of different experimental approaches used in this work are presented.

3.1. Experimental setups

Experiments for this work were run in three different experimental cells, and two setups.

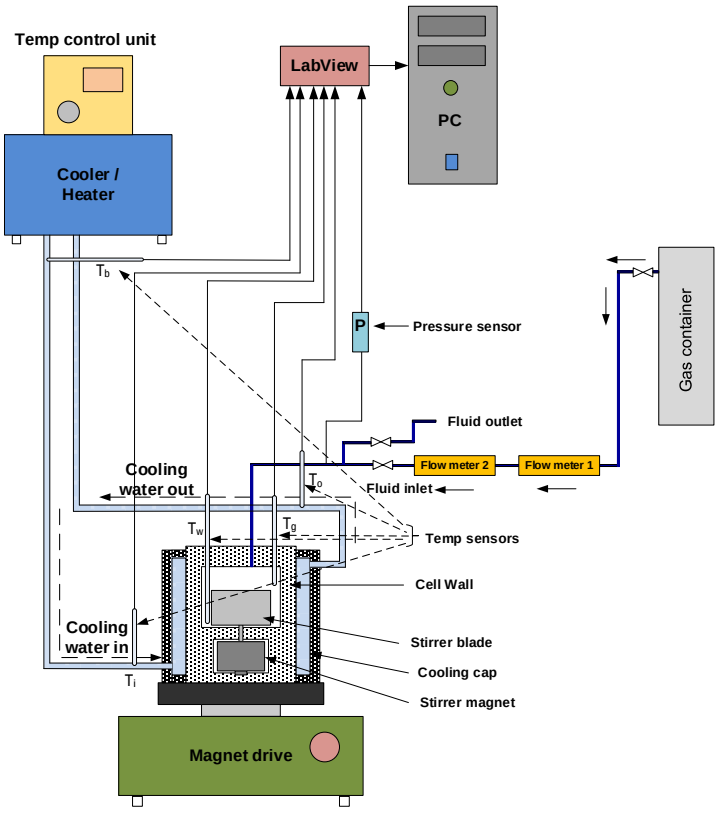

Figure 8. Experimental set-up.

3.1.1. Growth kinetics experiments

The growth kinetics experiments were conducted in two autoclave cells of similar design, but different diameters. Pictured in **Figure 7**, the set-up includes a gas container for gas supply during hydrate growth to maintain cell pressure constant. A Bronkhorst HIGH-TECH flow meter is connected in the line between the gas container and the reactor cell, for measuring gas flow rate into the cell during hydrate growth. Two 1/10 DIN Pt-100 temperature sensors (accuracy ± 0.03 °C) are installed through the top lid of the cell to enable temperature monitoring in the gas and bulk phase during experiments. Pressure monitoring is enabled using a Rosemount 3051TA absolute pressure transmitter connected to the line along the inlet to the cell. To enable circulation of cooling fluid, a coolant jacket, envelops the cell body. Cooling and temperature control is enabled using a Julabo High Tech Series F34-HL refrigerating / heating circulator. The coolant used is water.

The cell sizes were 141.4 mL with a diameter of 60 mm, and 318.1 mL with a diameter of 90 mm. A detailed description of the cell dimensions has been presented in Paper V. The 141.4 ml cell is equipped with a second top lid, which has a sapphire window at center (insight diameter is 30 mm) as shown in **Figure 9**A. The other without a window, but with two temperature sensors for the gas phase at top of the cell and the water phase at the cell bottom is shown in **Figure 9**B. Stirring was enabled using a magnetic stirrer drive on which the cell was seated. The magnetic stirrer drive activates the stirrer magnet which seats in the lower chamber of the reactor cell, and is attached to a single flat blade impeller. The mixing power was measured using a RHODE & SCHWARZ HM8115-2 Power Meter.

3.1.2. Heat transfer experiments

The heat transfer experiments were conducted using mainly the 141.4 mL cell, with a few tests conducted in the 314.2 mL cell. Other tests for observation of gas hydrate structure and stability where also conducted in a 23 mL sapphire tube cell (Figure **10**). The sapphire window top lid (see Figure **9**A) was used with the 141.4 ml cell to study development of hydrate layer on the cell wall during heat transfer experiments with THF and ethylene oxide (EO) at atmospheric pressure. There was no need for gas supply or flow measurements during the heat transfer experiments, thus those components of the set-up were not engaged.

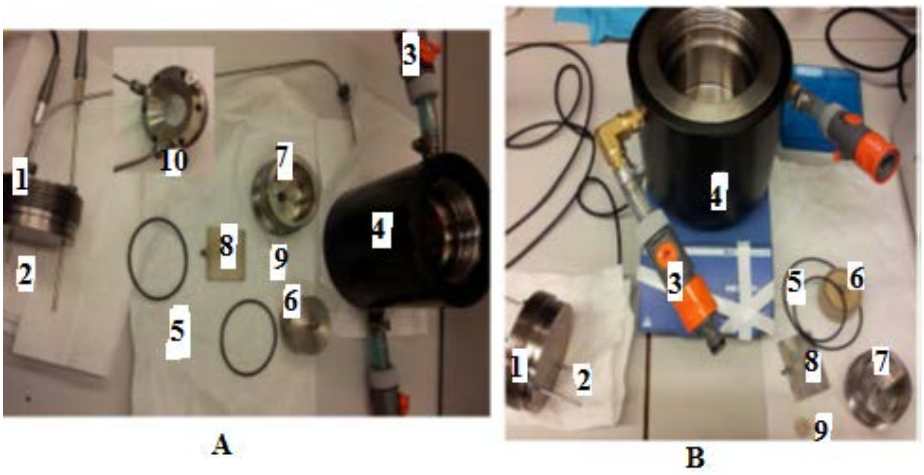

Figure 9. *Component parts of the titanium autoclave cells. 1 is top lid, 2 are the temperature sensors, 3 is connection for cooling fluid circulation through the cell with a stop valve, 4 is main cell body, 5 are O-ring ceilings for top and bottom lid, 6 is the magnet holder, 7 is the bottom lid, 8 is the stirrer blade, 9 is plastic ring for reduction of friction between magnet and cell, and 10 is an extra top lid with a sapphire window.*

Figure 10. *Components of the 23mL sapphire cell. 1 is the top lid with pressure and temperature sensors, 2 are the O-ring ceilings, 3 is protective cap, 4 is connection between bottom lid and sapphire cell, 5 is bottom lid, 6 is sapphire tube (cell), 7 is magnet holder, 8 is stirrer blade*.

3.2. Experimental procedure

3.2.1. Methane hydrate - growth kinetics experiments

All experiments were run at a pressure of 90 bars. The cell content was cooled down at constant cooling rate of 3°C/h from an initial temperature of 13.5°C to the required experimental temperature. System pressure was maintained constant at 90 bar within a deviance of ±2 bar, by adding "fresh" methane from the gas container through the flow meter.

The cell is first cleansed and washed with tap water, then rinsed thoroughly with distilled water. The housing around the stirrer magnet is filled with distilled water to remove residual air, and the reaction chamber is filled with the required volume of distilled water for the test and the cell is closed by mounting the top lid.

The autoclave cell is then purged twice with methane gas to 40 bars, to remove residual air from the reaction chamber prior to charging with gas to the experimental pressure of 90 bars. The methane hydrate equilibrium temperature

at 90 bar is approx. 12 °C. During charging the cell temperature is adjusted to 13.5 °C, to keep the cell outside the hydrate region prior to start of experiment.

Starting at 13.5 °C the cooling bath is programmed to maintain this temperature constant for 10 minutes for the cell to equilibrate before start of cooling. Then the cell is cooled down to the experimental temperature without stirring at a cooling rate of 3 °C/h. When the cell has reached the desired experimental temperature the stirrer is started at the desired stirring rate. The stirring system is automated so that the magnetic stirrer automatically turns off upon start of cooling, and starts again when the system has reached the required experimental temperature. The back pressure valve connecting the 2 liter gas container to the autoclave reactor cell is adjusted to maintain constant cell pressure during the course of an experiment. Hydrate formation is gauged by monitoring the gas flow through a flow meter in the line between the 2 liter gas container and the autoclave reactor cell. Gas flow along with cell pressure, temperature, and stirring rate is read using LabVIEW(R). After each experiment the autoclave cell is cleaned by first dissociating the hydrate through pressure depletion and heating in a controlled manner, after which it is washed clean with distilled water and kept ready for the next experiment.

3.2.2. Heat transfer experiments

A series of heat transfer experiments have been conducted using 3 different gas hydrate formers, methane; Tetrahydrofuran (THF); and Ethylene Oxide (EO). Gas hydrate had to be formed first, followed by heat transfer tests. Methane is a gas at experimental conditions, while THF and EO can be kept in liquid form and are soluble in water. So the approach used for methane hydrate was different from that used for THF and EO hydrates.

3.2.2.1. Procedure with methane as hydrate former

Cell preparation and filling are done in similar steps as outlined for the growth kinetics experiments. Upon complete hydrate formation (taken at about 3 hours from onset of growth), the cell is locked in with the pressure at 90 bars, and heat transfer tests are conducted via cooling – heating cycles of 8°C – 4°C – 8°C (**Figure 11**). Heat transfer tests were conducted for 5, 10. 20, 40, and 60% hydrate content. The hydrate concentration was reduced in steps by controlled dissociation followed by pressure depletion, with the final cell pressure approximately 90 bars at each concentration considered during the heat transfer tests. It must be noted though the uncertainty in determining the exact hydrate content through this method, as at the given pressure the system lay within the hydrate formation region. Thus there might have been cases of some hydrate formation / dissociation during the cooling / heating cycles. The need for better control of the hydrate content in the cell prompted the use of THF and EO which are soluble in water at our experimental conditions.

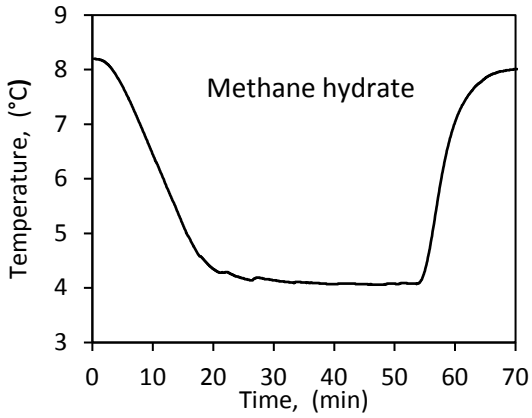

Figure 11.Heat transfer tests, cooling - heating and heating - cooling circles for methane hydrate.

3.2.2.2. Procedure with THF and EO as hydrate former

Both THF and EO are miscible with water, so it was easy to control the amount of hydrate formed by adding stoichiometric portions of each to the cell pre-filled with the desired amount of water. The stoichiometric combining ratios of THF and EO with water to form 1 unit mole of hydrate is 1:17 and 3:23 respectively. These ratios represent 100% hydrate formed in this work, while lower concentrations are taken as fractions of this ratio. Experiments were conducted for 0, 10, 20, 40, 60, 80, and 100% hydrate. A tabular presentation of the volume, and mass of THF and EO added at the different concentrations is presented in Paper IV.

While THF is a liquid at standard conditions, EO has boiling point at 10.7 °C at atmospheric pressure and thus needs to be cooled down to liquid form before required amounts are measured out for the experiments. This is done by cooling down the EO fluid released from the low pressure EO liquid containing cylinder into a tubing which is soaked into an ice bath (**Figure 12**). The experimental procedure was in the following steps:

- Hydrate formation is preceded by filling the cell with the required amount of water, and cooling down the cell to about 6^{o}C.
- The required volume of liquid THF or EO oxide is then added. This was done directly via an air nob on the top lid of the cell for THF, while the cell was moved into the fume cupboard containing the EO cylinder where EO is added to the cell content. Note: EO and THF are toxic if inhaled or absorbed into the skin.

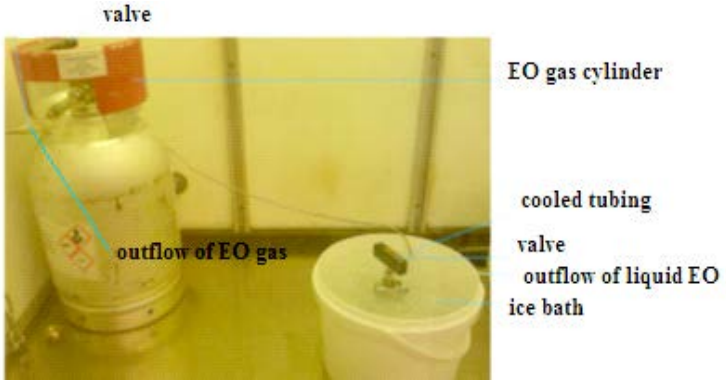

Figure 12. Ethylene oxide gas is cooled down to liquid form

- The cell is tightly shut and hydrate is formed via constant cooling, while stirring the cell content. The cell is cooled down to 1^{o}C. Complete hydrate formation is assumed after 3 to 5 hours from onset of hydrate growth.
- Next heat transfer tests are performed: Heating – cooling cycles of 1^{o}C – 4^{o}C – 1^{o}C, with and without stirring. (**Figure 13**)

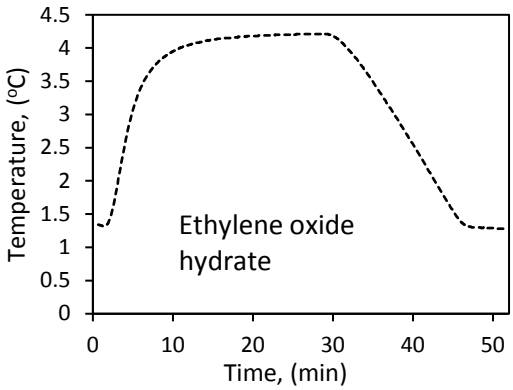

Figure 13.Heat transfer tests, cooling - heating and heating - cooling circles for ethylene oxide hydrate.

4. Modeling hydrate growth from heat transfer

Chapter 4 describes the essence and purpose of the modeling approach used in our studies.

4.1. Background

We have seen from chapter 1 that established knowledge ascribes gas hydrate growth kinetics to three main mechanisms, intrinsic kinetics; mass transfer; and heat transfer. Each of these mechanisms contribute to hydrate formation kinetics, depending on the hydrate forming system. A number of works, including those by Vysniauskas and Bishnoi [41], Englezos et al. [52], and Lekvam and Ruoff [70] have modeled gas hydrate growth based on intrinsic kinetics. Intrinsic kinetics models usually link the nucleation rate to the growth via particle size distributions, which require in-situ measurements via imaging techniques like Nuclear Magnetic Resonance (NMR) and Raman Spectroscopy [58].

Mass transfer also plays an important role in hydrate growth kinetics. For hydrates to form, there must be a transport of guest molecules to the reaction interface, usually the point at which the concentration of guest molecules is highest; the gas-liquid interface [121-123]. Mass transfer based models describe gas hydrate growth kinetics as a function of the mass transport of gas molecules across the gas – liquid interface. The Skoveborg and Rasmussen model [59] and the model by Herri et al. [124] are examples of attempts to model gas hydrate growth based on mass transfer.

The third controlling mechanism for gas hydrate growth, heat transfer, has been focused on in this work. Gas hydrates have been found to form at the coldest spots on pipe walls, due to favorable heat transfer [125]. When gas

hydrates form, the temperature of the hydrate crystal surface rises towards the equilibrium temperature, and the released heat is absorbed into the surrounding medium, usually a mixture of hydrate, water, and gas [62, 126]. The heat released into the hydrate forming environment must be effectively removed for hydrate formation to continue [19]. Continued hydrate growth is enabled due to the absorption of the produced heat by the surrounding fluids, water and gas, away from the crystal surface. This naturally leads to an increased temperature in the gas and water phases.

Observations in our laboratory have shown that the degree of temperature increase in the cell is proportional to the amount of hydrate produced. Such accumulated heat in the reactor would slow down the growth rate of hydrate crystals because of a reduction in effective driving force of the system. Thus a good balance between microscopic heat transfer from the crystal surface as described in the models on the growth of hydrate film front [61-64], and macroscopic heat transfer from the reactor volume is essential to the hydrate growth kinetics.

4.2. Heat transfer model

In this work, we present a heat transfer model based on fundamental theory. The model enabled us analyze important factors that affect the heat transfer process during hydrate growth, and the growth kinetics.

4.2.1. Model development

In the present study, hydrate growth has been considered as a crystallization process with heat transfer as the governing mechanism. The model is based on the following assumptions:

1) The heat released from hydrate formation is transferred to the hydrate-water-gas mix (assumed to be homogeneous) in the reactor,

2) A part of this heat is transferred to the circulating coolant through the reactor wall,

3) The remaining part of the heat is absorbed by the hydrate-water-gas mix and results in an increase in temperature,

4) The temperature increases to an optimal level producing a temperature gradient where the heat transfer across the reactor wall balances the heat production due to hydrate growth. (**Figure 14**)

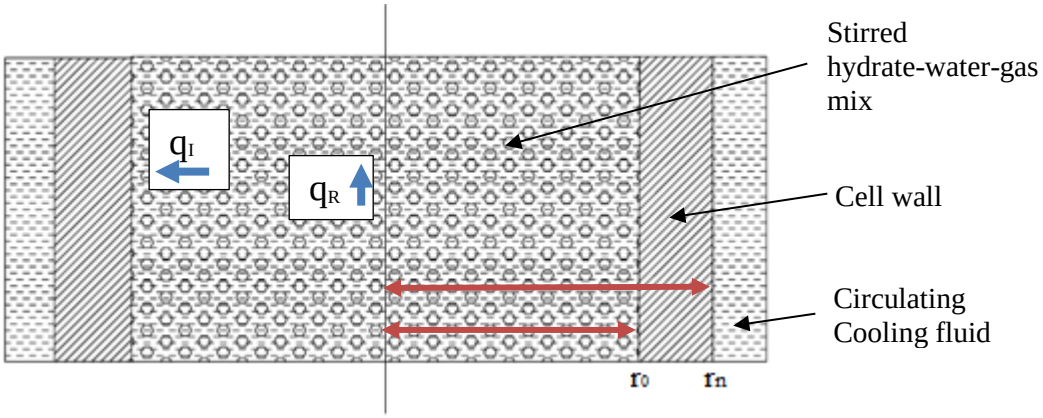

Figure 14. A vertical slice of reactor system, with reaction products, hydrate-water-gas in a homogeneous mix. Heat produced from hydrate growth (q_R) is released into the system mix, some of which is transferred out through the cell wall (q_I).

Growth is thus considered to commence with a visible spike in the cell temperature. The temperature signature in the cell as growth progresses would be indicative of the growth rate, through a balance between the heat removed by the coolant circulating through the cooling jacket, and the heat produced as hydrates form. This is a macroscopic representation of the process, thus the model presents the global growth rate within the system and not growth on the surface of individual hydrate nuclei / particles in the solution.

Depending on the process (endothermic or exothermic), the energy absorbed by a unit mole of the reactants, or released by a unit mole the products in the form of heat, is equal to the enthalpy of formation ΔH. Gas hydrate formation being an exothermic process is associated with heat release. Data given by Anderson [120], Handa [127], and Gupta [128], puts the enthalpy of methane hydrate formation at approximately 54 KJ/mole.

In our system, during hydrate growth the heat balance may be seen across 3 boundaries (**Figure 15**):

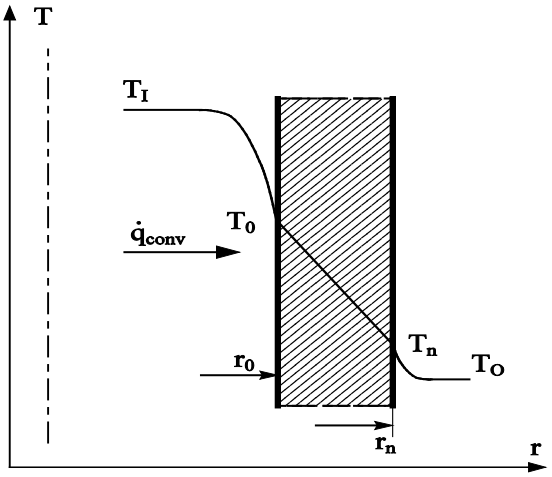

Figure 15. Convection border conditions.

1. The cell interior: where the heat released from hydrate growth is dispersed. Aided by the stirring of the cell content, the heat produced is assumed to be uniformly distributed within the cell volume into the gas – water – hydrate mix. Heat produced from hydrate formation per unit time would be

$$\dot{q}_R = \frac{dn}{dt} \cdot \Delta H_{gen} \tag{20}$$

where:

$\dot{q}_R$ is the rate of heat generation from hydrate formation [J/s],
dn/dt is the gas consumption rate [mole/s],
and ΔH_{gen} is the enthalpy of hydrate generation [J/mole].
But the heat is actively being removed from the cell interior into the other two boundaries, the cell wall and the coolant flux, which allows for continued hydrate growth. The heat produced from hydrate formation will then be equal to the heat the heat transfer from the cell interior (via convection) plus the heat absorbed by the gas – water – hydrate mix (the sensible heat increase)

$$\dot{q}_R = h_I \cdot A_I \cdot (T_I - T_0) + \frac{d(c_p \cdot m \cdot T_I)}{dt} \tag{21}$$

where h_I is the heat transfer coefficient from the reactor interior to the reactor wall, A_I is the heat transfer area, T_I and T_0 are the interior and wall temperatures in the reactor, c_p is the specific heat capacity of the reactor mix, and m is the mass of the reactor mix.

Combining equations (20) and (21), we get

$$\frac{dn}{dt} = \frac{1}{\Delta H_{gen}} \cdot \left[h_I \cdot A_I \cdot (T_I - T_0) + \frac{d(c_p \cdot m \cdot T_I)}{dt} \right] \tag{22}$$

The product $c_p \times m$ is the thermal mass of the cell content, it is an additive property

$$c_p \cdot m(t) = c_{p,H} \cdot m_H(t) + c_{p,w} \cdot m_w(t) + c_{p,g} \cdot N_g(t) \tag{23}$$

The specific heat capacities of the different phases are assumed constant within the temperature range in the cell. The following values have been used: Water, c_w = 4200 J/kg K; Hydrate, c_H = 2100 J/kg K; Gas (CH_4), $c_{p,g}$ = 49.26 J/mole K.

2. At the cell wall: Heat from the cell interior is conducted through the cell wall, and can be formulated from the Fourier equation. This will depend on the thermal conductivity of the cell wall material, and the temperature gradient across the cell wall. Simply put

$$q_r = h_I \cdot (T_I - T_0) = -\alpha \cdot \frac{dT_w}{dr} \qquad (24)$$

where α is the thermal conductivity of the reactor wall material, and dT_w/dr is the temperature gradient across the reactor wall, with wall thickness dr.

3. The coolant flux: carries the transferred heat from the cell away. Thereby giving enough local subcooling in the cell for continued hydrate growth. The heat transfer coefficient for the coolant flux (h_O) is estimated using the dimensionless Nusselt number approach [129]. h_O is required as an input value for estimating the outer cell wall temperature – Paper I.

For a thick walled reactor, there is a transient temperature profile across the reactor wall, which changes as a function of the temperature in the cell, T_I, and the temperature of the coolant, T_O (**Figure 15**). Thus, a transient temperature profile must be solve for each border condition.

Discretizing, explicit for time derivative:

1. For the cell interior

$$T_I^{p+1} = \frac{\left[\dot{q}_R - 2h_I \cdot (\pi\delta r_0) \cdot \left(T_I^p - T_0^p\right)\right] \cdot \Delta t}{\left(c_{p,H} \cdot m_H(t) + c_{p,w} \cdot m_w(t) + c_{p,g} \cdot N_g(t)\right)} + T_I^p \tag{25}$$

If there is no hydrate formation, $\dot{q}_R$ = 0, then

$$T_I^{p+1} = \frac{\left[-2h_I \cdot (\pi\delta r_0) \cdot \left(T_I^p - T_0^p\right)\right] \cdot \Delta t}{\left(c_{p,H} \cdot m_H(t) + c_{p,w} \cdot m_w(t) + c_{p,g} \cdot N_g(t)\right)} + T_I^p \tag{26}$$

2. At the cell wall

inner border (i = 0)

$$T_0^{p+1} = \frac{2h_I\Delta t}{\rho c\Delta r}\left(T_I^p - T_0^p\right) + \frac{2\alpha\Delta t}{r_0(\Delta r)^2} \cdot \left(r_O + \frac{\Delta r}{2}\right) \cdot \left(T_I^p - T_0^p\right) + T_0^p \tag{27}$$

interior node i

$$T_i^{p+1} = T_i^P + \frac{\alpha\Delta t}{(\Delta r)^2} \cdot \left(T_{i+1}^P - 2T_i^p + T_{i-1}^P\right) + \frac{\alpha\Delta t}{2r_i\Delta r} \cdot \left(T_{i+1}^P - T_{i-1}^P\right) \tag{28}$$

outer border

$$T_n^{p+1} = \frac{2h_O\Delta t}{\rho c\Delta r}\left(T_O^p - T_n^p\right) + \frac{2\alpha\Delta t}{r_n(\Delta r)^2} \cdot \left(r_n + \frac{\Delta r}{2}\right) \cdot \left(T_n^p - T_{n-1}^p\right) + T_n^p \tag{29}$$

The equations can be solved for two different scenarios: 1) with T_I as the unknown parameter, and h_I as a fitted parameter; 2) with $\dot{q}_R$ as the unknown parameter, while h_I is a predetermined input variable and the system temperature is known from measurements. In the cases with hydrate growth (Paper III), h_I is first determined using scenario 1, then $\dot{q}_R$ is determined using scenario 2. The h_I values are estimated using scenario 1, in the cases when we performed heat transfer studies for different hydrate content in the hydrate – water slurry.

It is important to stress that the model has been formulated in a very simplified form to allow for easy computation, and comes with some obvious limitations. Firstly, the heat transfer is considered only in the radial direction; neglecting possible heat transfer into the cell from the top lid depending on the temperature in the room, and from the bottom lid due to mechanical heat produced by the stirrer motor. Secondly, the thermal mass changes during hydrate growth. To calculate the thermal mass requires that one keeps track of the gas consumption rate for hydrate formation, which also allows for accounting for the change in water and hydrate phases during hydrate growth. However, the need for knowing the gas consumption rate for hydrate formation limits the model to give just empirical estimates.

Where the heat transfer from the cell is efficient enough, depending on the heat release rate, there would be no accumulation of heat within the cell interior. This may be obtainable for scaled-up reactors, and would allow for a more massive production of gas hydrates.

5. Results and discussion

In studying hydrate growth kinetics we have performed several experiments with 3 hydrate formers, methane gas a sI hydrate former; Ethylene Oxide (EO) also a sI hydrate former; and Tetrahydrofuran (THF) a sII hydrate former.

The results are presented in three subsections below. First we present our findings on:

- how temperature, water content, stirring rate, and reactor size affect the gas hydrate growth kinetics,
- the effect of gas hydrate content on heat transfer, and
- how heat transfer impacts gas hydrate growth kinetics.

The main results are summarized and discussed in this section to address the main project objectives. Detailed results and discussion are presented in the enclosed papers.

5.1. Effect of different parameters on methane hydrate growth kinetics

The effects of temperature, water content (which reflects hydrodynamic parameters such as mean bubble and droplet sizes), agitation, as well as reactor size on gas hydrate growth kinetics have been studied. The findings from these studies are important for better gas hydrate management practices in flow assurance. In addition, the development of new gas hydrate based technologies introduced in section 1.3.3, require very rapid and efficient gas/water conversion rates to hydrate. These studies give new insight on how the

parameters investigated affect the growth rate of hydrate, in a semi-batched autoclave reactor.

The growth kinetics in our system consists of three different and characteristic stages, stage-I, stage-II, and stage-III, dependent on the growth dynamics in the cell (**Figure 16**). Prior to hydrate growth onset, we have the induction period, once the system attains a constant super saturation marked by a constant temperature in the cell from the start of stirring. During this time, the nucleation process is ongoing, with the system attempting to form a critical cluster size for spontaneous growth of gas hydrate. Hydrate growth onset is characterized by a rapid increase in temperature above the initial experimental temperature, due to the release of the enthalpy of phase transition [21].

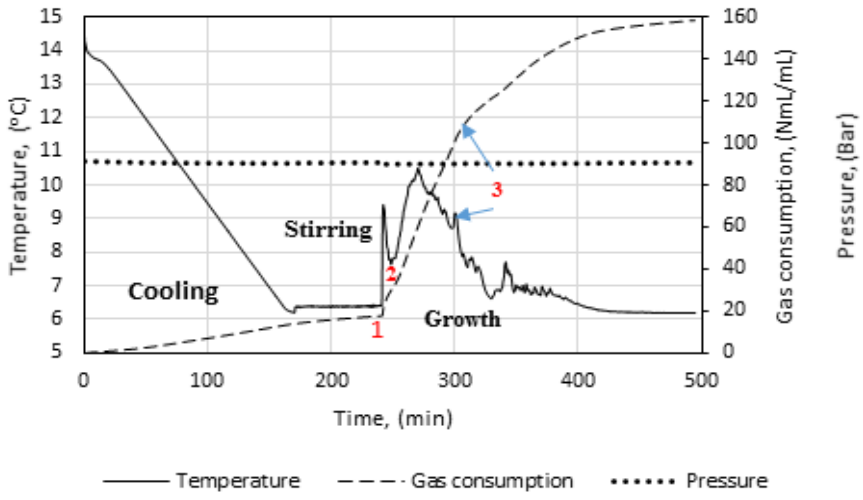

Figure 16. Pressure, temperature, and gas consumption data from a typical experimental run (141.4 mL cell, 50 mL water).

The growth stages are distinguished by an obvious change in the growth rates as shown in **Figure 16**; with stage-I between points 1 – 2, stage-II between points 2 – 3, and the lowest growth rate at the third and terminal stage-III from

point 3. Some authors have reported similar growth trends in their works [22, 52]. In the work by Englezos et al. [52], the end of growth stage-I was identified as the turbidity point; the point at which the hydrate crystals formed become visible. Observations from this work indicate that at the end of stage-I, significant amount of hydrate crystal is already formed in the cell. The amount of water converted to hydrate at the end of growth stage-I was between 2 – 5% for most experiments, but there were cases when the value was much lower or on the contrary, higher. On average, more water was converted to hydrate during stage I as the initial volume of water in the cell increased. At 50 mL initial water content, 500 rpm, and 6°C, we had the lowest water converted to hydrate of about 0.21% during stage I. On the other hand, at 50 mL initial water content, 700 rpm, and 8°C, we had the highest water converted to hydrate of about 9.14% during stage I. (Paper V) The clear trend in increased water converted to hydrate with increasing water content during stage I, may be explained from amount of gas that presaturates the system prior to hydrate formation. Given that more methane gas is dissolved in the system with higher water content, more water is converted during spontaneous hydrate growth at growth onset in stage I.

In Paper V we have discussed how the growth rate during stage I is strongly affected by the water content, stirring rate, and the temperature of the system. Lower temperatures and higher stirring rates led to an increase in gas consumption rate. However, higher water content led to a decrease in gas consumption rate. Solubility of methane increases with decreasing temperature in the absence of hydrate [130], therefore more gas is dissolved prior to hydrate formation at lower temperatures, which partly explains the higher average gas consumption rate with decreasing temperature during stage I. From the response of gas consumption with decreasing temperature, and the amount of gas consumed with increasing water content during stage I, we can deduce that

the gas initially consumed during growth stage I is mainly the dissolved gas that saturated the water phase before growth commenced. Thus, the intrinsic kinetics mechanisms discussed in section 1.2.2., may play a dominant role in the growth kinetics during stage I. As **Figure 17** shows, the gas consumption during stage I is a non-linear function of time, which agrees with the inference drawn from equ (18) in section 1.2.2. that this is reflective of a crystal growth process controlled by intrinsic kinetics [48].

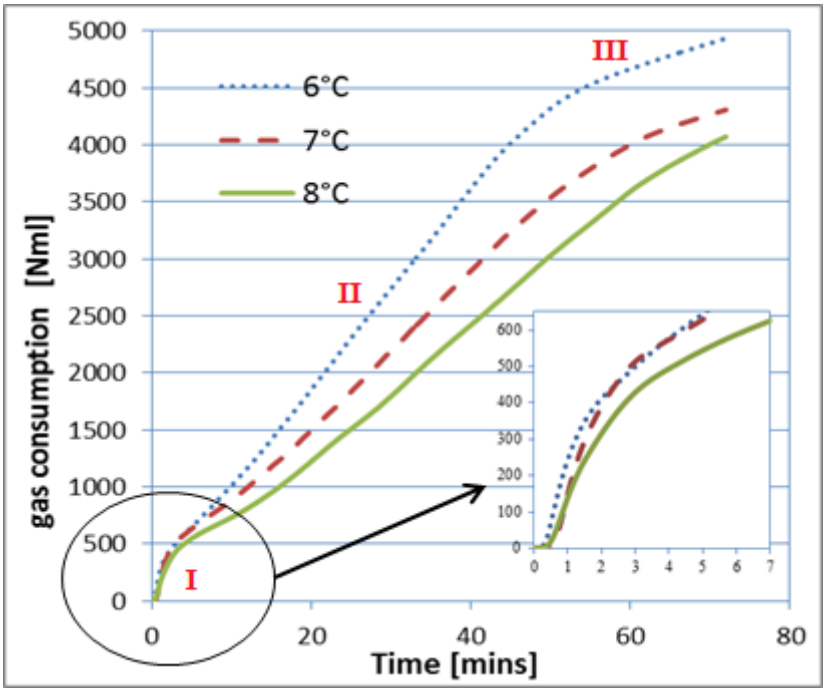

Figure 17. Gas consumption profile showing different hydrate growth stages, at 6 (dots), 7 (dashes) and 8 °C (whole line) versus time (50ml water content, 700rpm stirring rate).

Stage II starts with a dip in the cell temperature, which reflects the change in the growth mechanism. The initially dissolved methane gas has been

converted to hydrate during stage I, and now the amount of gas available in the bulk phase for hydrate crystallization depends on the rate of transport of gas across the gas – liquid interface. Hashemi et al. [54] showed that the rate of gas dissolution into the bulk phase (k_La) is an order of magnitude lower than the rate of gas inclusion into the growing hydrate crystal (k_ra_s). Thus no matter how fast gas molecules are being included into the growing crystal structure, the rate of hydrate formation will be limited by the gas dissolution rate. This also means that the contribution of gas dissolution to the gas consumption during hydrate growth is negligible, and thus, the overall gas hydrate growth rate can simply be represented by the gas consumption rate.

The initial dip in temperature at the start of stage II indicates that momentarily, less heat of hydrate formation is being released compared with stage I. i.e. the hydrate growth rate has decreased during stage II. Since heat has accumulated in the cell, as evident from the temperature rise, other secondary effects such as an increased mass transfer barrier due to poorer gas – liquid mixing, a drop in the effective solubility of the gas, and increase in the viscosity of the gas – hydrate – water slurry. This effect is compounded by a further build up in the cell temperature due to an increase in the heat transfer resistance due to hydrate build up in the cell. We see that the gas consumption is roughly a linear function of time during growth stage II. At stage III the cell is plugged from agglomerated hydrate mass, and not representative of the growth kinetics. Growth stage-II is where the highest amount of gas is consumed, and is more representative of the overall kinetics of the process. Thus focus is placed on growth data from stage-II, which is used for extensive analysis on the hydrate growth kinetics in our further discussions of the results in this work. Paper II and Paper V give further discussion on the processes impacting the different growth stages.

5.1.1. Effect of temperature (subcooling)

The equilibrium curve on **Figure 18** indicates the theoretical region of hydrate formation for the experimental pressure of 90 bars. Although gas hydrates should form from about 11.9 ^{o}C at 90 bars, most laboratory systems require cooling down by some degree below the equilibrium temperature for hydrates to form. As we go from laboratory to industrial size scale, hydrates tend to form closer to the equilibrium temperature most probably due to the increased volume and contact area between water and gas and a corresponding increase of the probability of nucleation [32]. This probably offers some explanation for why Mork and Gudmundsson reported that subcooling had no impact on the rate of hydrate formation for both a pure methane, and a hydrocarbon gas mixture [46, 47].

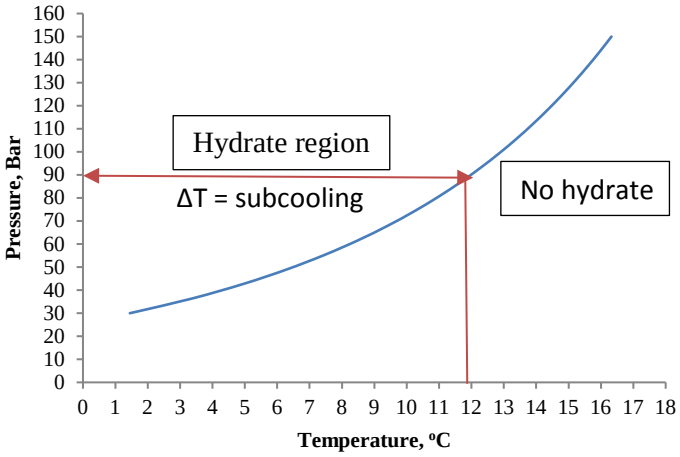

Figure 18. Methane Hydrate Equilibrium Curve (Calculated with CSMGem Software).

Various contrasting findings have been reported on the effect of increasing subcooling / decreasing temperature on the growth rate of gas hydrates. Takahata et al. [75] reported a decrease in the apparent and specific mass

transfer coefficient with a decrease in temperature, for kinetics studies performed on methane hydrate. For studies on CO_2 gas hydrate kinetics Clarke and Bishnoi [58] reported an increase in apparent mass transfer coefficient with a decrease in temperature, while the intrinsic rate constant did not show a clear relationship with temperature. Meanwhile, the works by Mori [62], and Mochizuki and Mori [126] reported an increase in the lateral growth rate of CO_2 and Methane hydrate films with an increase in subcooling. Peng et al. [131] also observed an increase in hydrate film growth rate with an increase in subcooling for a gas bubble suspended in a water droplet. Other works that were carried out in stirred tank reactors at constant pressure, by Vysniauskas and Bishnoi [41], and Happel et al. [132] showed an increase in hydrate growth rate with an increase in subcooling. Results from this work, shown in **Figure 19**, indicate that methane hydrate growth rate progressively increased as the temperature was decreased from 8, 7, to 6 ^{o}C. The increase in the growth rate with decreasing temperature may be directly related to an increase in the subcooling or temperature driving force [133].

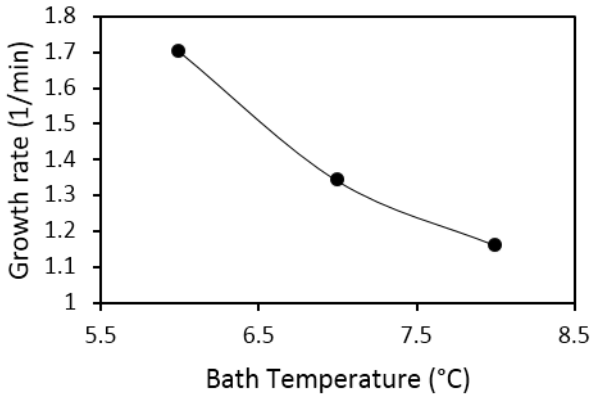

Figure 19. Effect of temperature on gas hydrate growth rate.

5.1.2 Water content

The amount of water in a system plays a role in the formation kinetics of gas hydrates. In systems where the water volume is very low, such that the water is completely dispersed in the oil or gas phase, though hydrates form, there may be no risk of plugging, if the hydrate particles would be carried along with the flowing stream. We have not found many works focused on the subject, but have reason to suggest that there may be a positive correlation between the amount of water in a flowline in which hydrate forms and the probability of plugging. Joshi et al. [134] performed flow loop experiments for a high water cut system, in which he suggests that at high liquid loadings (50% water and above), plugging occurred at the same hydrate fraction irrespective of the liquid loading of the system. One must note though that the mixing velocities for which the results were presented were not the same. The mixing velocity was higher for the case with a higher liquid loading. Further results from the same work showed that the system would plug at a lower hydrate fraction with higher liquid loading, for the same mixing velocity [134]; supporting the argument that the probability of plugging may correlate positively with the amount of water in the system. The reason for this correlation may be because, the absolute volume of hydrates formed is higher at higher liquid loading, which increases the available hydrate particles for agglomeration and eventual plugging.

The effect of water content is also important to industrial scale hydrate production, where the focus is both on quantity, which require large liquid volumes, and rapid production rates. **Figure 20** shows results from this work, where gas hydrate growth rate decreased with an increase in water content, dropping by about 50%. Reasons for this include hydrodynamic factors such as: 1) the turbulence energy dissipated into the system is higher at lower water content - Paper V, 2) increased gas recirculation at lower water content which

strongly promotes the gas-liquid mass transfer of the system [135], 3) lower droplet and bubble sizes at lower water content which increases the gas-liquid contact area.

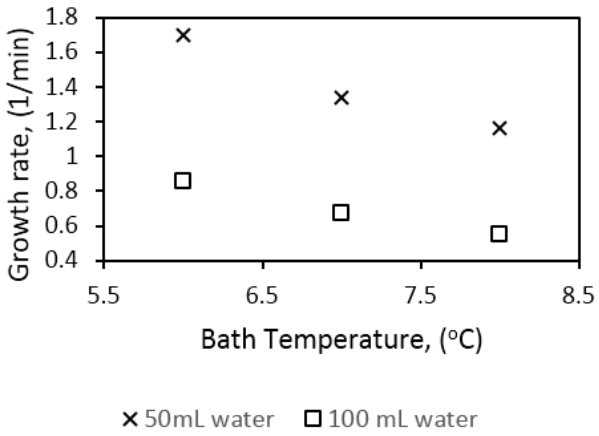

Figure 20. Effect of water content on hydrate growth (700 rpm).

5.1.3. Stirring rate (degree of agitation)

The use of stirring is common in industrial processes for enhances reaction kinetics [60, 135, 136]. Stirring enhances the mixing, mass transfer, and heat transfer, all contributing to promote the reaction rate. Similarly, stirring has been used as a means for promotion of hydrate formation [74, 75, 137], and has also been useful for faster hydrate dissociation in our laboratory. However, in industrial processes one must reach a balance between the energy input into a process, and the gains in product output, for the process to be considered feasible. Increased stirring rate increases the power consumption. Thus it is of concern, what degree of stirring or agitation will be adequate to optimize the output of the process. For gas hydrate formation processes, stirring significantly reduces the induction time and increases the growth rate [29, 138]. This observation is explained by an increase in collision rate, increased bubble

concentration in the water phase (i.e. increased amount of gas dispersed and available for the reaction); and an increase in gas-liquid contact area, as the bubble size decreases with stirring. [32, 139] This results in a more dispersed and finely mixed system.

The findings from our work indicate that the effect of stirring rate on the growth rate partly depends on the mechanism that controls the growth process. For example, during stage-I the growth rate progressively increased with an increase in the stirring rate. The growth during stage-I is partly from gas that had already dissolved, and supersaturates the system prior to growth onset. Thus we assume negligible mass transfer restriction during stage I. In addition, growth stage-I is so brief that we can assume that the rapid rise in temperature during this period would not impact the growth kinetics. Therefore we suggest that the controlling mechanism during growth stage-I is the intrinsic kinetics. At growth stage-II, mass transfer and heat transfer restrictions begin to play a more significant role. As seen from **Figure 16**, the temperature builds up even more during growth stage-II, causing a drop in the temperature driving force. In addition the presence of hydrate crystals increases the viscosity of the mixture and impairs both the mass transfer and heat transfer out of the cell.

Figure 21 shows the growth rates for stirring rates of 350 rpm to 1200 rpm at experimental temperatures of 8, 7, and 6 ^{o}C. The growth rate seems to peak between 500 and 575 rpm, beyond which additional increase in the stirring rate does not improve the growth rate. Other related works have argued that the stirring rate beyond which there is no further promotional effect on the growth rate indicates that the stirring rate is high enough to consider further heat and mass transfer enhancement negligible [52, 58]. It is important to plan rapid hydrate production processes with such an optimal stirring rate, for energy efficiency. As we will see in the next subsection (section 5.1.4), a similar trend is observed with stirring, upon scale-up.

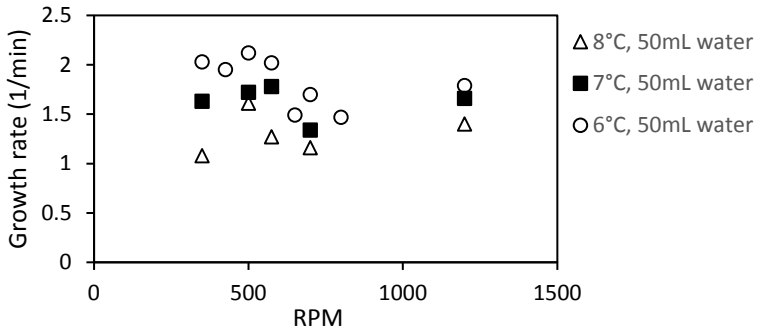

Figure 21. Effect of stirring rate on growth rate in 141.4 mL cell (50mL water content).

5.1.4. Reactor size

Size scale is an important factor in reactor experiments. In moving from laboratory to industrial scale, certain scaling factors are taken into consideration in other to maintain the credibility and transferability of results to a larger scale. Experiments were performed in a "small cell" with a volume of 141.4 mL, and a "large cell" with a volume of 318.1 mL. Both cells are geometrically similar, details of the cell design are given in *Table **1***.

Table 1. Details of Autoclaves used in this work.

Cell volume, mL	**141.4**	**318.1**
Reaction chamber height, H, m	0.05	0.05
Reaction chamber diameter, D_R, m	0.06	0.09
Impeller diameter, D_I, m	0.045	0.062
Impeller height, H_I, m	0.045	0.045
Volume of liquid, $V_L \times 10^3$, m^3	0.05, 0.1	0.1125, 0.225
Volume of gas, $V_G \times 10^3$, m^3	0.0914, 0.0414	0.2056, 0.0931
V_G/V_L	1.828, 0.414	1.828, 0.414
Liquid height, H_L , m	0.0177, 0.0354	0.0177, 0.0354
Material	Titanium	Titanium

Scale-up of dispersion systems as we have in this work aims at maintaining: 1) hydrodynamic similarity; and 2) constant heat transfer capacity. To maintain hydrodynamic similarity, it is recommended to keep the impeller tip speed and/or Reynold's number, impeller power consumption per unit volume of liquid, gas / liquid volume ratio, liquid / tank height ratio, impeller / tank diameter ratio, and gas-liquid interfacial area constant, among others [47, 140]. From Table 1 we see that geometrical scale-up incorporates all the parameters related to the reactor size. We have as well kept the gas / liquid volume ratio constant in this work. The scaling factors for maintaining hydrodynamic similarity are also crucial to maintaining constant heat transfer capacity, in addition to the heat transfer area per unit volume of the reactor [141].

Figure 22 shows that more gas is consumed with scale-up, because there are more reacting volumes of gas and water at a larger scale. However, when we normalize the growth rates by the initial volume of water available for hydrate

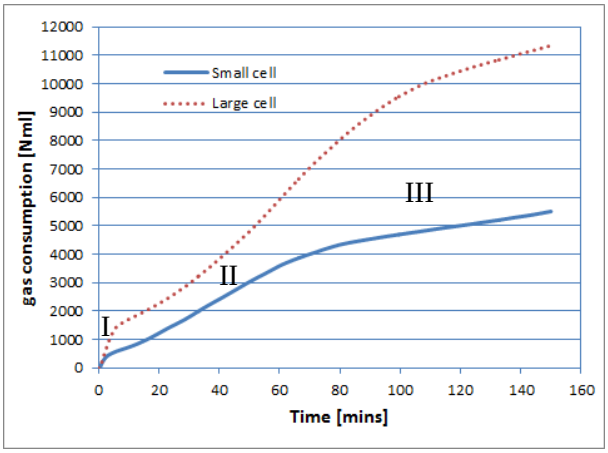

Figure 22. Influence of reactor size (diameter) on gas hydrate growth (gas consumption is not normalised by the volume of water in the reactor). The water content in the cell was kept at a value that reflected comparable gas / water volume ratios in both cells. Tests conditions are 8°C, and 700rpm.

formation, as seen from **Figure 23**, the growth rate drops significantly with scale up, even at lower subcooling values.

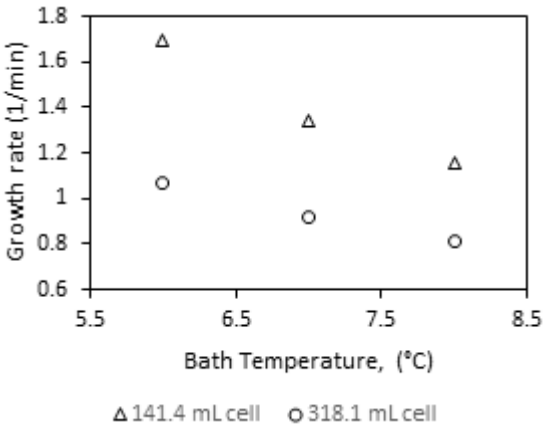

Figure 23. Effect of reactor size on gas hydrate growth at different experimental temperatures (700 rpm).

Mori [141], suggested that to maintain a constant hydrate forming capacity in stirred tank reactors (normalized per unit volume of the reactor) that are scaled-up with geometric similarity, requires an increase in the power input per unit volume (P_{mix}/V) in proportion to the reactor diameter (D_R) to the power higher than 3.2 but less than 8. Mori further argues that for scale-up with geometric similarity, a constant power input per unit volume will be identical to the relation $(P_{mix}/V) \propto D_R^3$, and thus fails to provide sufficient power for maintaining the hydrate forming capacity per unit volume constant. **Figure 24** shows plots of the growth rate versus the mean bubble size (d_b), impeller Reynold's number (N_{Re}), impeller tip velocity (U_{TIP}), and impeller power consumption per unit volume liquid in the cell (P_{mix}/V). The mean bubble diameter was estimated using the correlation for the average bubble diameter from literature, based on isotropic turbulence theory for estimating the average

bubble size [142]. We see that similar to the response with stirring rate, the growth rate plateaus at certain value, where further increase d_b, N_{Re}, U_{TIP}, and P_{mix}/V does not increase the growth rate. Moreover, at similar Reynold's number, impeller tip velocity, mean bubble diameter, and power input per unit volume, the growth rate per unit volume is less with scale-up.

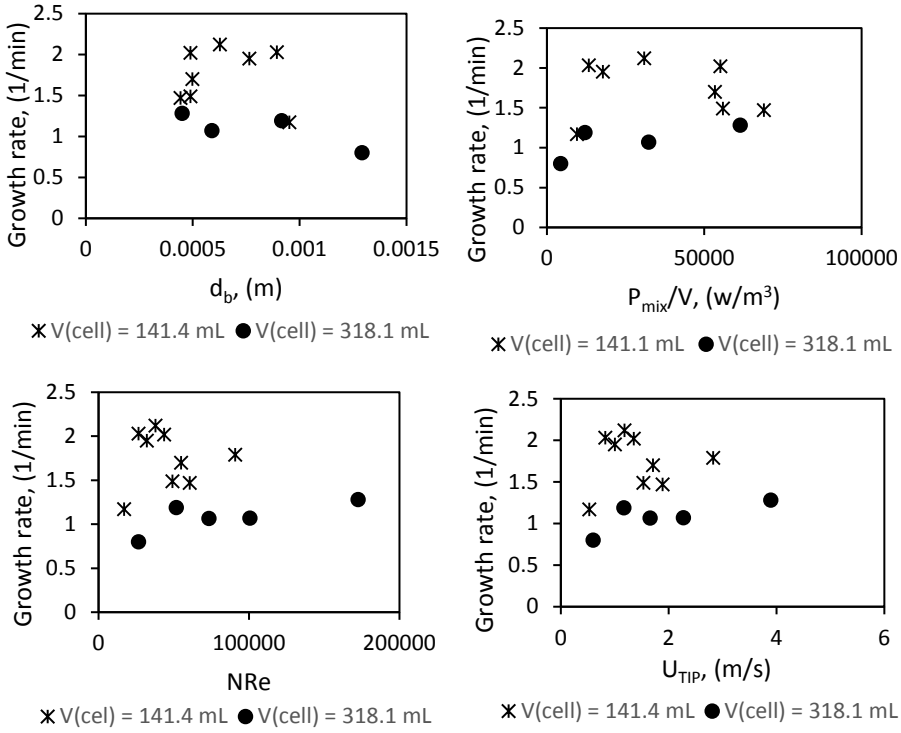

Figure 24. Hydrate growth rate as a function of d_b, N_{Re}, U_{TIP}, and P/V in the 141.4mL and 318.1mL cells (6°C).

The fact that increasing power input per unit volume does not lead to a further increase in the growth rate once the rate has plateaued brings to question Mori's argument on insufficient power input per unit volume as being the reason for lower gas hydrate formation capacity upon scale-up. On the other hand, for scale-up with geometric similarity, the specific surface area for heat

transfer will be equal to $4/D_R$. This means that the specific thermal conductance is lower for scale-up with geometric similarity, an argument supported by the analysis by Nauman [143]. If this decreased specific thermal conductance accounts for the lower growth rates upon scale-up, then efforts should be directed at increasing the driving force for heat transfer upon scale-up while keeping geometric similarity intact. Some recommendations on how to maintain the thermal conductance upon scale-up and to enhance heat transfer from the reactor are discussed in the work by Nauman [143], and others [129, 144].

Recent works have shown that increasing the degree of dispersion of the liquid phase itself will greatly enhance the gas – liquid mass transfer [145-148], and substantially improve heat and mass transfer during hydrate growth [149]. Batched and Semi-batched stirred tank reactors have the water and hydrate mixed within the reactor in volumes that limit the degree of dispersion obtainable, which creates a limit to the heat and mass transfer in the reactor, and this effect increases with an increase in reactor size.

5.2. Effect of hydrate content on heat transfer

Gas hydrates form in production, transportation, and process facilities, where they deposit on walls and surfaces of their containing vessels and may lead to plugging [125]. Gas hydrates are also know to form in reservoir sediments [90, 150-152], and other natural environments. The formation of hydrates in such systems would lead to an alteration of the heat transfer behavior through them. This observation is reasonable, since the heat transfer properties of gas hydrates differs from those of water, gas, and petroleum [153-155], and the reservoir matrix.

Part of the work in this PhD project has been focused on the effect of hydrate content on heat transfer. Studies were initially done with methane hydrate (Paper I), with variations in methane hydrate content of 5%, 10%, 20%, 40%, and 60%. Results revealed that heat transfer decreased with an increase in methane hydrate content in the hydrate-water slurry (see **Figure 25**). A similar observation is made by Liu et al. in another work [156]. Note, that the methane hydrate studies were done under quiescent conditions (without stirring), which reflects the heat transport in reservoir sediments. The thermal conductivity of methane hydrate was estimated at 60% hydrate content, as equal to 0.45 w/m/K. This falls within 75% of values previously published using other methods [157, 158].

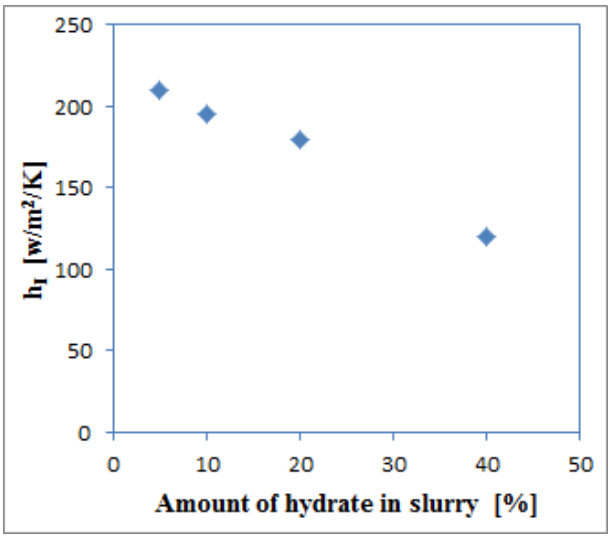

Figure 25. Heat transfer coefficient (h_l) through methane hydrate slurry, as a function of hydrate concentration in slurry.

Heat transfer in flowing systems is usually associated with turbulence, which was not reflected in the methane hydrate studies. Thus additional studies

were carried out with Tetrahydrofuran (THF) and Ethylene oxide (EO) hydrates. THF and EO hydrates offer the advantage of better control over the amount of hydrate formed in the cell, and enabling stirring during the heat transfer tests without altering the hydrate content much. Tests were carried out with THF and EO solute concentrations of 10%, 20%, 40%, 60%, 80%, and 100%. These concentration would represent the maximum concentrations of hydrate in the hydrate – water slurry, where 100% represents a stoichiometric mixture of the hydrate former with water (Paper IV).

Experimentally observed hydrate equilibrium temperatures in our cell indicated that the hydrate equilibrium temperature, T_{eq}, of EO and THF systems containing less than 100 % of stoichiometric solution was reduced compared to the 100 % solution. The reduction in T_{eq} increased with the reduction of % concentration of solute in the solution. T_{eq} at 20% solute in the solution was 2°C for EO and -0.5°C for THF. Thus, at the lower THF and EO concentrations (less than 40%) the hydrate amount could still be affected to some degree by the temperature in the cell during the heating / cooling test. The observed hydrate structures during the heating/cooling tests at 1°C and 4°C for 20% EO and THF concentration indicate that there was still some hydrate at both temperatures, in the 141.4 mL titanium cell. However, the structure was less compact at 4°C, indicating some dissociation. No visible hydrates were observed at both temperatures for 10% solute concentration. Our observations in the 23mL sapphire cell showed no visible THF hydrate structure at 20% solute concentration for both temperatures, indicating that the hydrates are less stable in smaller reactors.

In these studies we investigated the effect of hydrate content with and without stirring. The effect of stirring rate and cell size were also studied. Our findings also shed light on the deposition behavior of hydrates on the cell wall.

5.2.1. Effect of hydrate content

The effect of hydrate content on the heat transfer indicates a possible structural influence. Heat transfer decreased with an increase in hydrate content up to the point at which the cell content turned from slurry to solid hydrate deposited on the cell wall. Beyond this point (at about 40 - 60% hydrate content) the heat transfer remained fairly constant as shown in **Figure 26**. However, we observe a jump in the heat transfer coefficient for Ethylene oxide hydrate (EO) once the hydrate concentration reaches 60% and the heat transfer coefficient reached a level above that in system without hydrate. This deviates from the normal trend of decreasing heat transfer coefficient with an increase in hydrate content, and we haven't yet found a reasonable explanation for this observation.

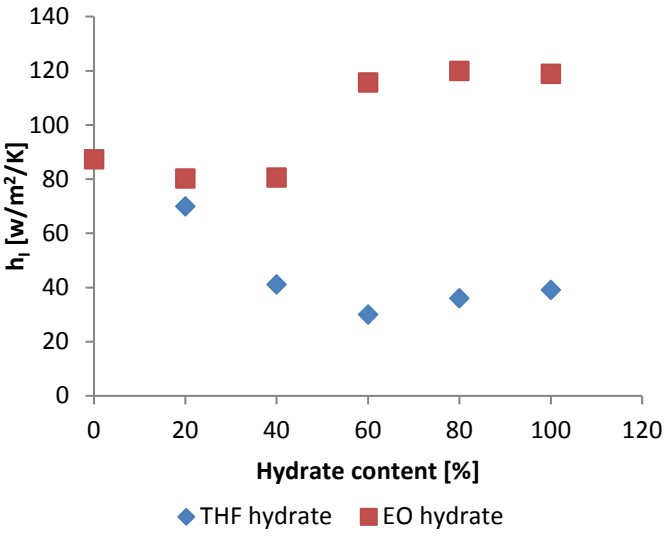

Figure 26. Internal heat transfer coefficient as a function of THF and Ethylene oxide hydrate concentration (No stirring).

A few inferences may be made from the results. First, the thermal properties of gas hydrates in the presence of other mediums are additive, giving rise to the

progressive decrease in heat transfer with increasing hydrate content in the slurry [2]. When the hydrate mass becomes solid, the dominant heat transfer mechanism becomes heat conduction, instead of convection. It appears that at about 60% guest content, the hydrate crystal assumes a stable solid structure, with identical thermal properties to the structure formed at maximum cavity filling (**Figure 27**). At 40-60% hydrate content, we were guaranteed hydrate would deposit on the wall, which is synonymous to plugging in pipe flow. Though other research works have recorded cases of pipeline plugging at hydrate contents as low as 4% [159]; raising a question as to what drives plugging in pipelines in case of hydrate formation?

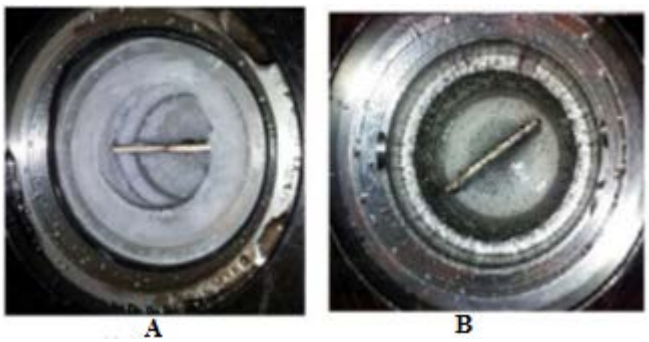

Figure 27. Gas hydrate structure in cell, A - solid hydrate layer deposited on the reactor wall (>= 40%); and B - Hydrate still in slurry form (< 40%).

The results further establish the fact that the presence of hydrates in reservoir sediments would change the thermal properties of the system [90, 91], but also, different hydrate contents would vary the degree of alteration of the thermal state of the reservoir system.

The same would be the case for flowing pipeline or well systems with hydrate present in them. The heat transfer restriction out of the system will increase with hydrate content. In the following section we analyze the impact

of turbulence created by stirring on the heat transfer in hydrate containing systems [125].

5.2.2. Effect of stirring

Heat transfer tests were run at stirring rates of 500 and 1000 rpm, and compared with the case without stirring. Stirring the cell content enhanced the heat transfer in general, but an optimal heat transfer rate was obtained at 500 rpm. **Figure 28** shows that stirring enhanced heat transfer for the THF hydrate system, but the degree of heat transfer enhancement with stirring decreased with an increase in hydrate content, for up to 40% hydrate content or less. Above this concentration, the effect of stirring on the heat transfer was negligible.

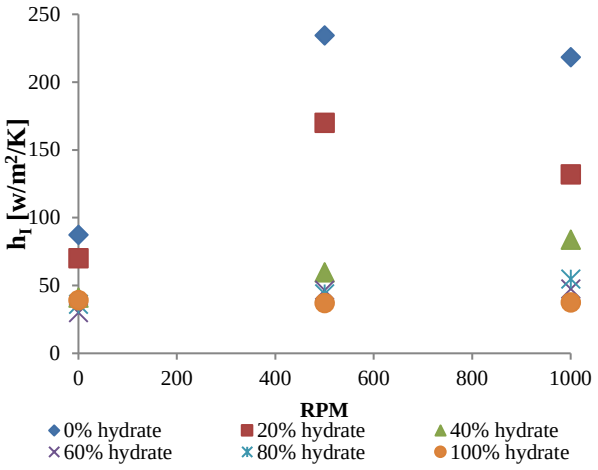

Figure 28. Effect of stirring on the heat transfer through THF hydrate slurry, at different hydrate concentrations.

The case with EO hydrate showed some unexpected differences in the heat transfer response with stirring (**Figure 29**). Heat transfer enhancement was only observed between 0 - 20% hydrate content. While between 40 – 100% hydrate content, heat transfer rather decreased with stirring. We know that a solid

hydrate layer was already deposited on the cell wall from 40% EO hydrate content. Given that EO hydrate is stable at a much higher temperature (approx. 11°C at 100% and 9°C at 40% solute concentration), it would have a higher compaction at the heat transfer test conditions, but it is unclear how this may relate to the drop in heat transfer at these hydrate content levels.

Observations from the cell temperature profile indicated that after a solid hydrate layer was deposited on the cell wall, stirring the cell content led to heat production in the cell. Such heat production which may be due to lattice vibration will have a dulling effect on the effective heat transport through the hydrate layer, and we see this as a drop in heat transfer coefficient.

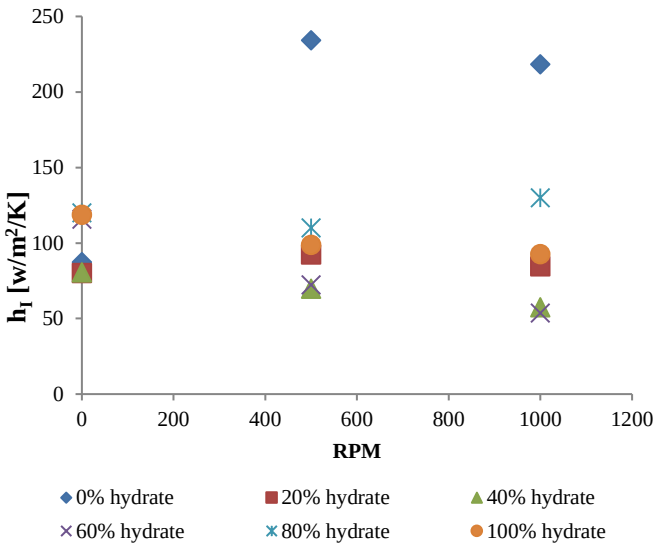

Figure 29. Effect of stirring on the heat transfer through Ethylene oxide hydrate slurry, at different hydrate concentrations.

We can directly relate the heat transfer response with stirring to the form of hydrate in the cell. When the hydrate was in slurry form, stirring enhanced the heat transfer, while there was no enhancement in heat transfer when a solid

hydrate mass was formed. The response with stirring also indicates that hydrate formed in the cell did not dissociate much with stirring even at solute concentrations below 40%.

5.3. Heat transfer in gas hydrate growth kinetics

In the previous sections we observed that the heat transfer through hydrate slurry decreases as the amount of hydrate content increases. We also noted that stirring the cell content immensely improves the heat transfer out of the cell [160, 161], even with hydrate present (Paper IV) [162]. However, these observations were made under static conditions, with strict control on the amount of hydrate in the cell. Conversely, real time hydrate formation is a dynamic process that involves online hydrate formation with turbulence or agitation. During hydrate growth the hydrate content steadily increases, while flowing conditions ensure mixing of the stream phases and possible turbulence. Consider a time clip of a flowing stream with formed hydrate particles as illustrated in **Figure 30**. Then, assuming the hydrate particles flow along with the fluid at the same speed (constant speed / velocity), the development of the flow and the hydrate concentration changes with time. The hydrate concentration continues to increase, as more hydrate is formed, while the turbulence in the system gradually damps with time. Next we consider the effect of heat transfer on hydrate growth kinetics in a dynamic system, as a time dependent process.

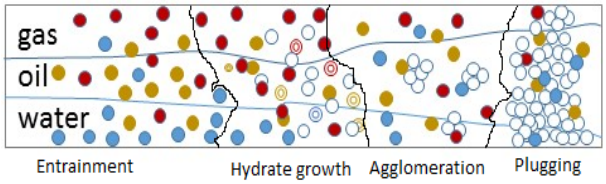

Figure 30. A time frame of hydrate formation in a flowing stream (Picture taken from [20], courtesy of [7]).

Some key factors when modeling hydrate growth based on heat transfer are amongst others identified to be the hydrate content, and the heat transfer coefficient. The different growth stages as hydrate growth progresses characterize different regions of approximately constant heat transfer coefficients within each region. **Figure 31** shows that the system temperature can be predicted by the model if the input heat transfer coefficient is optimized to a new value with each characteristic growth stage. The estimated values of the heat transfer coefficient h_I, shows a similar trend to those observed from previous works under static conditions. The heat transfer starts out quite high during stage I of hydrate growth with less than 10% hydrate content, but progressively decreases as hydrate growth continues.

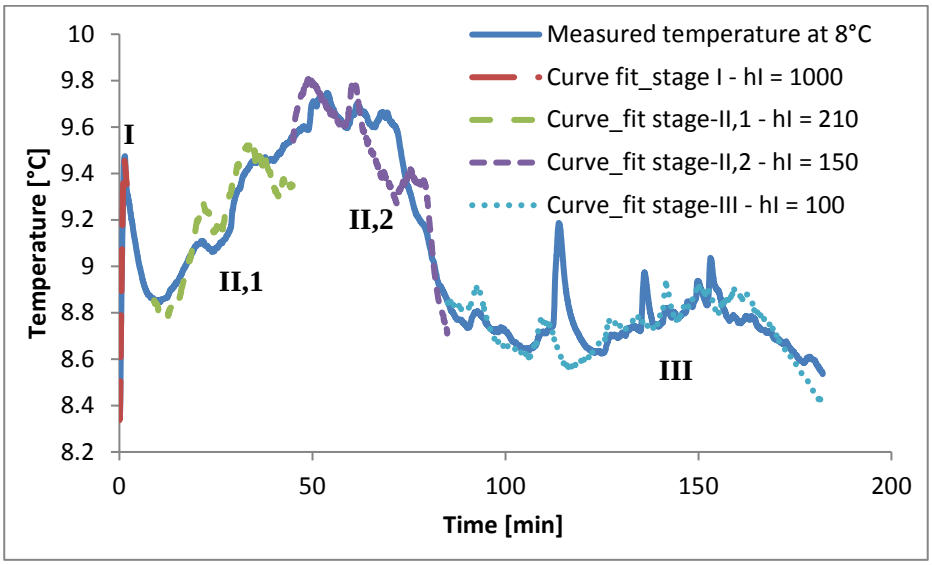

Figure 31. Temperature fit - with different values of h_I over 4 distinct growth regions spread across growth stages (I, II, and III).

The decrease in h_I with time is directly related to the increase in hydrate content in the cell, as well as changes in flow behavior in the cell induced by changes in rheology of the cell content with time due to hydrate accumulation [163]. It is noteworthy that the heat transfer coefficient during hydrate growth is transient, and dependent on the amount of hydrate formed; though rough averages have been taken over time periods corresponding to each growth stage. Thus, in modeling hydrate growth based on heat transfer, the transient nature of the heat transfer coefficient should be considered.

5.3.1. Estimating hydrate growth based on heat transfer

Estimated values of h_I from the temperature fit were used as an input to the heat transfer model to estimate the heat production rate during hydrate growth. Gas consumption was estimated from the heat produced as

$$Gas\ consumption = \frac{\dot{q}_R \cdot V_n \cdot \Delta t}{\Delta H_{gen}} \tag{30}$$

where $\dot{q}_R$ is the heat production rate from hydrate formation, V_n is the molar volume of gas at normal conditions (24024 NmL/mole), ΔH is the enthalpy of hydrate formation (54 [KJ/mole methane consumed] for methane hydrate), and Δt is the time step. **Figure 32** and **Figure 33** show plots of the simulated gas consumption compared with the measured gas consumption during growth stage II. This stage is representative of the normal growth kinetics in our reactor.

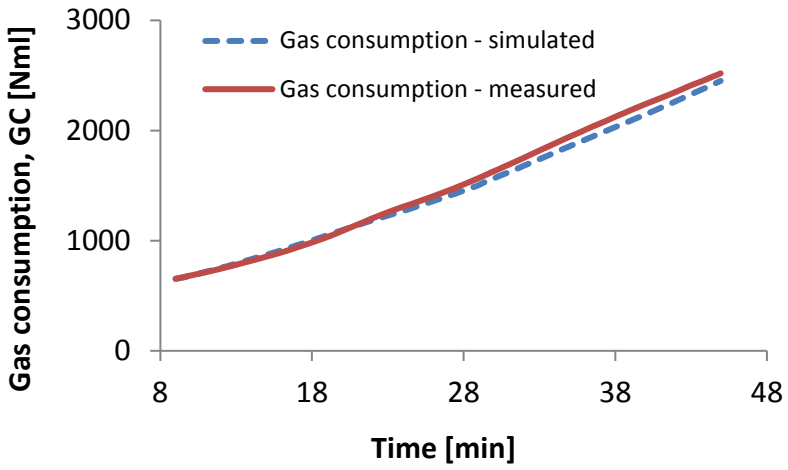

Figure 32. Comparing simulated and measured gas consumption during hydrate growth stage-II,1 (first segment).

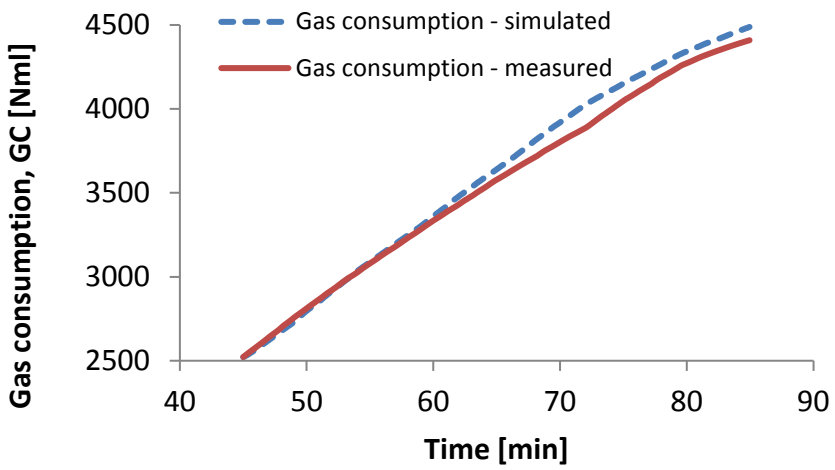

Figure 33. Comparing simulated and measured gas consumption during hydrate growth stage-II,2 (second segment).

By determining the average values of the heat transfer coefficients for each growth segment we could get (obtain) a good match of simulated gas consumption data, compared with the experimental data. Noteworthy, it was impossible to get a good fit for all stages of hydrate growth with a single heat transfer coefficient value (Paper III) [71], further stressing the need for taking into account the transient nature of the heat transfer coefficient when modelling gas hydrate growth based on heat transfer. A number of studies have suggested that at high enough stirring rates, the heat and mass transfer resistance can be rendered negligible [52, 58]. But this is clearly system dependent [65, 66]. The results presented in the present work are for a stirring rate of 700 rpm. We consider the effect of heat and mass transfer to be negligible from 500 rpm and above. Other results from our laboratory indicated that increasing the stirring rate from 500 to 1000 rpm did not increase the heat transfer through hydrate slurry, but rather dulled the heat transfer rate (see **Figure 28** and **Figure 29**).

6. Conclusions and future works

In this section, the overall conclusions from this study are addressed. Recommendations for the future work are also suggested. During this PhD work we have performed several experiments using distilled water with methane gas, Tetrahydrofuran (THF), and ethylene oxide (EO) as hydrate formers; in autoclave stirred tank reactors.

6.1. Conclusions

The results from the work on hydrate growth kinetics lead to the following conclusions:

- Increasing subcooling / decreasing system temperature strongly increased the gas hydrate growth rate. This was mainly due to the increase in the temperature driving force.

- Increase of water content by an approx. factor of 2 gave almost a reduction of growth rate by a factor of 2. This is clearly due to hydrodynamic effects such as higher gas dispersed into the bulk, smaller average bubble diameter, and better gas recirculation at a lower water content.

- The effect of stirring rate depends on the controlling mechanism of hydrate growth. During growth stage-I, when growth was primarily controlled by intrinsic kinetics, the growth rate progressively increased with increasing stirring rate. During growth stage-II, when the growth was primarily controlled by mass and heat transfer, the growth rate plateaued when the stirring rate ensured negligible mass and heat transfer restriction, and the

heat transfer rate out of the cell reaches equilibrium with the rate of heat production from hydrate formation.

- Scaling up reactor size with geometric similarity lead to an increase in the absolute volumes of hydrate formed, but almost a halving of the hydrate formation capacity per unit volume. The drop in hydrate formation capacity seems to be primarily due to a decrease in the specific thermal conductance of the reactor and heat and mass transfer limitations created by the limit to the degree of the liquid phase dispersion in batched and semi-batched stirred tank reactors as we scale-up. Thus, for hydrate production purposes, it is suggested to take measures to maintain the driving force of heat transfer while maintaining geometric similarity (if possible) with scale-up.

The results from the work on heat transfer in connection with hydrate growth lead to the following conclusions:

- The global hydrate growth rate can be described by heat transfer model provided the effect of hydrate concentration on heat transfer is considered.

- The heat transfer through hydrate slurry decreases with an increase in the hydrate content.

- Gas hydrate forms a solid deposit on the reactor wall at concentrations high enough for coagulation into a solid mass. This occurred between 40 – 60% hydrate content.

- The heat transfer through hydrate mass remained constant once a solid wall deposit was formed.

- The heat transfer through the hydrate slurry was significantly higher with stirring when the slurry could still flow.

- Heat transfer through the hydrate slurry also plateaued at a given stirring rate, since there was no additional increase in the heat transfer coefficient when the stirring rate was increased from 500 rpm to 1000 rpm.

- The transient nature of the heat transfer coefficient must be considered when modeling gas hydrate growth based on heat transfer.

6.2. Future works

Hydrate growth estimation based on heat transfer

The current heat transfer model assumes heat transfer in the radial direction only. This simplification does not take into consideration possible heat transfer in the axial direction through the top and bottom lids of the reactor. Thus it would be a good continuation of this work to extent the model to heat flow in the axial direction as well.

The wall temperatures have been estimated from numerical solutions interpolating from average outer and inner cell temperatures. We now have designed a new cell with increased radius and volume (same height), with modifications that allow for direct measurements of the outer and inner cell wall temperatures. Temperature sensors at the top and bottom surfaces are also included. This will enable measurements of the heat flux through the cell in all

directions and will reduce uncertainties associated with estimating the heat transfer coefficients to a large extent.

Hydrate growth kinetics

The results analysis shows that the growth rate at the onset of growth, i.e. growth stage I is largely from dissolved gas that pre-saturates the system, and is not representative of the dominant growth kinetics of the system. However, some hydrate is formed during growth stage I, which further impacts the growth kinetics during stage II. An interesting future work could be to establish an experimental procedure that enables instantaneous hydrate formation, and cuts out the growth stage-I and the possible effects that accompany it. We believe this will substantially increase the average growth rate.

7. References

1.Israelachvili, J.N., *Intermolecular and Surface Forces: Revised Third Edition*. Academic press,2011.

2.Sloan Jr, E.D. and Koh, C., *Clathrate Hydrates of Natural Gases*. CRC press,2007.

3.Sloan, E.D., Koh, C.A., and Sum, A., *Natural Gas Hydrates in Flow Assurance*. Gulf Professional Publishing,2010.

4.Sloan, E.D., Fundamental Principles and Applications of Natural Gas Hydrates. *Nature*, **2003**. *426*(6964): p. 353-363.

5.Sloan, E.D., A Changing Hydrate Paradigm—from Apprehension to Avoidance to Risk Management. *Fluid Phase Equilib.*, **2005**. *228*: p. 67-74.

6.Koh, C.A. and Sloan, E.D., Natural Gas Hydrates: Recent Advances and Challenges in Energy and Environmental Applications. *AlChE J.*, **2007**. *53*(7): p. 1636-1643.

7.Zerpa, L.E., Salager, J.-L., Koh, C.A., Sloan, E.D., and Sum, A.K., Surface Chemistry and Gas Hydrates in Flow Assurance. *Industrial & Engineering Chemistry Research*, **2011**. *50*(1): p. 188-197.

8.Kvenvolden, K.A., Gas Hydrates-Geological Perspective and Global Change. *Reviews of geophysics-richmond Virginia then Washington*, **1993**. *31*: p. 173-173.

9.Collett, T.S., Energy Resource Potential of Natural Gas Hydrates. *AAPG bulletin*, **2002**. *86*(11): p. 1971-1992.

10.Makogon, Y., Holditch, S., and Makogon, T., Natural Gas-Hydrates—a Potential Energy Source for the 21st Century. *Journal of Petroleum Science and Engineering*, **2007**. *56*(1): p. 14-31.

11.Makogon, Y.F., Natural Gas Hydrates–a Promising Source of Energy. *Journal of Natural Gas Science and Engineering*, **2010**. *2*(1): p. 49-59.

12.Olah, G.A., Beyond Oil and Gas: The Methanol Economy. *Angew. Chem. Int. Ed.*, **2005**. *44*(18): p. 2636-2639.

13.Tajima, H., Yamasaki, A., and Kiyono, F., Energy Consumption Estimation for Greenhouse Gas Separation Processes by Clathrate Hydrate Formation. *Energy*, **2004**. *29*(11): p. 1713-1729.

14.Aaron, D. and Tsouris, C., Separation of CO_2 from Flue Gas: A Review. *Sep. Sci. Technol.*, **2005**. *40*(1-3): p. 321-348.

15.Eslamimanesh, A., Mohammadi, A.H., Richon, D., Naidoo, P., and Ramjugernath, D., Application of Gas Hydrate Formation in Separation Processes: A Review of Experimental Studies. *J. Chem. Thermodyn.*, **2012**. *46*: p. 62-71.

16.Duc, N.H., Chauvy, F., and Herri, J.-M., CO_2 Capture by Hydrate Crystallization–a Potential Solution for Gas Emission of Steelmaking Industry. *Energy Convers. Manage.*, **2007**. *48*(4): p. 1313-1322.

17.Komatsu, H., Ota, M., Smith, R.L., and Inomata, H., Review of CO_2–Ch 4 Clathrate Hydrate Replacement Reaction Laboratory Studies–Properties and Kinetics. *Journal of the Taiwan Institute of Chemical Engineers*, **2013**. *44*(4): p. 517-537.

18.Mullin, J.W., *Crystallization*. Butterworth-Heinemann,2001.

19.Ribeiro, C.P. and Lage, P.L., Modelling of Hydrate Formation Kinetics: State-of-the-Art and Future Directions. *Chem. Eng. Sci.*, **2008**. *63*(8): p. 2007-2034.

20.Meindinyo, R.-E.T. and Svartås, T.M., Intermolecular Forces in Clathrate Hydrate Related Processes, in ASME 2015 34th International Conference on Ocean, Offshore and Arctic Engineering; American Society of Mechanical Engineers:2015.

21.Kashchiev, D. and Firoozabadi, A., Nucleation of Gas Hydrates. *J. Cryst. Growth*, **2002**. *243*(3): p. 476-489.

22.Abay, H.K. Kinetics of Gas Hydrate Nucleation and Growth. Ph. D. Thesis, University of Stavanger, Stavanger, Norway, 2011.

23.Parent, J. and Bishnoi, P., Investigations into the Nucleation Behaviour of Methane Gas Hydrates. *Chem. Eng. Commun.*, **1996**. *144*(1): p. 51-64.

24.Walsh, M.R., Koh, C.A., Sloan, E.D., Sum, A.K., and Wu, D.T., Microsecond Simulations of Spontaneous Methane Hydrate Nucleation and Growth. *Science*, **2009**. *326*(5956): p. 1095-1098.

25.Lee, K., Lee, S.-H., and Lee, W., Stochastic Nature of Carbon Dioxide Hydrate Induction Times in Na-Montmorillonite and Marine Sediment Suspensions. *International Journal of Greenhouse Gas Control*, **2013**. *14*: p. 15-24.

26.Krüger, S. and Deubener, J., Stochastic Nature of the Liquid-to-Crystal Heterogeneous Nucleation of Supercooled Lithium Disilicate Liquid. *J. Non-Cryst. Solids*, **2014**. *388*: p. 6-9.

27.Jiang, S. and ter Horst, J.H., Crystal Nucleation Rates from Probability Distributions of Induction Times. *Crystal Growth & Design*, **2010**. *11*(1): p. 256-261.

28.Ohmura, R., Ogawa, M., Yasuoka, K., and Mori, Y.H., Statistical Study of Clathrate-Hydrate Nucleation in a Water/Hydrochlorofluorocarbon System: Search for the Nature of the "Memory Effect". *The Journal of Physical Chemistry B*, **2003**. *107*(22): p. 5289-5293.

29.Skovborg, P., Ng, H., Rasmussen, P., and Mohn, U., Measurement of Induction Times for the Formation of Methane and Ethane Gas Hydrates. *Chem. Eng. Sci.*, **1993**. *48*(3): p. 445-453.

30.Natarajan, V., Bishnoi, P., and Kalogerakis, N., Induction Phenomena in Gas Hydrate Nucleation. *Chem. Eng. Sci.*, **1994**. *49*(13): p. 2075-2087.

31.Kashchiev, D. and Firoozabadi, A., Induction Time in Crystallization of Gas Hydrates. *J. Cryst. Growth*, **2003**. *250*(3): p. 499-515.

32.Svartaas, T.M., Ke, W., Tantciura, S., and Bratland, A.U., Maximum Likelihood Estimation a Reliable Statistical Method for Hydrate Nucleation Data Analysis. *Energy Fuels*, **2015**. *29*(12): p. 8195-8207.

33.Ke, W., Svartaas, T.M., Kvaløy, J.T., and Kosberg, B.R., Inhibition–Promotion: Dual Effects of Polyvinylpyrrolidone (Pvp) on Structure-Ii Hydrate Nucleation. *Energy & Fuels*, **2016**. *30*(9): p. 7646-7655.

34.Larsen, R., Lund, A., and Argo, C.B., Cold Flow-a Practical Solution, in Proc. of the 11th Int. Conf." Multiphase:2003.

35.Lund, A., Lysne, D., Larsen, R., and Hjarbo, K.W., *Method and System for Transporting a Flow of Fluid Hydrocarbons Containing Water*. 2004, Google Patents.

36.Larsen, R., Lund, A., Andersson, V., and Hjarbo, K., Conversion of Water to Hydrate Particles, in SPE Annual Technical Conference and Exhibition; Society of Petroleum Engineers:2001.

37.Makogon, I.U.r.F., *Hydrates of Natural Gas*. PennWell Books Tulsa, Okla, USA,1981.

38.Lederhos, J., Long, J., Sum, A., Christiansen, R., and Sloan, E., Effective Kinetic Inhibitors for Natural Gas Hydrates. *Chem. Eng. Sci.*, **1996**. *51*(8): p. 1221-1229.

39.Takeya, S., Hori, A., Hondoh, T., and Uchida, T., Freezing-Memory Effect of Water on Nucleation of CO_2 Hydrate Crystals. *The Journal of Physical Chemistry B*, **2000**. *104*(17): p. 4164-4168.

40.Buchanan, P., Soper, A.K., Thompson, H., Westacott, R.E., Creek, J.L., Hobson, G., and Koh, C.A., Search for Memory Effects in Methane Hydrate: Structure of Water before Hydrate Formation and after Hydrate Decomposition. *The Journal of chemical physics*, **2005**. *123*(16): p. 164507.

41.Vysniauskas, A. and Bishnoi, P., A Kinetic Study of Methane Hydrate Formation. *Chem. Eng. Sci.*, **1983**. *38*(7): p. 1061-1072.

42.Moudrakovski, I.L., Sanchez, A.A., Ratcliffe, C.I., and Ripmeester, J.A., Nucleation and Growth of Hydrates on Ice Surfaces: New Insights from 129xe Nmr Experiments with Hyperpolarized Xenon. *The Journal of Physical Chemistry B*, **2001**. *105*(49): p. 12338-12347.

43.Lee, J.D., Wu, H., and Englezos, P., Cationic Starches as Gas Hydrate Kinetic Inhibitors. *Chem. Eng. Sci.*, **2007**. *62*(23): p. 6548-6555.

44.Wu, Q. and Zhang, B., Memory Effect on the Pressure-Temperature Condition and Induction Time of Gas Hydrate Nucleation. *Journal of Natural Gas Chemistry*, **2010**. *19*(4): p. 446-451.

45.Wilson, P. and Haymet, A., Hydrate Formation and Re-Formation in Nucleating Thf/Water Mixtures Show No Evidence to Support a "Memory" Effect. *Chem. Eng. J.*, **2010**. *161*(1): p. 146-150.

46.Mork, M. and Gudmundsson, J.S., Hydrate Formation Rate in a Continuous Stirred Tank Reactor: Experimental Results and Bubble-to-Crystal Model, in Proceeding of the 4th International Conference on Gas Hydrates, Yokohama:2002.

47.Mork, M. Formation Rate of Natural Gas Hydrates - Reactor Experiments and Models. PhD Thesis, Norwegian University of Science and Technology, Norway, 2002.

48.Jensen, L. and von Solms, N. Experimental Investigation and Molecular Simulation of Gas Hydrates. PhD Thesis, Technical University of Denmark (DTU), Kgs. Lyngby, Denmark, 2010.

49.Noyes, A.A. and Whitney, W.R., The Rate of Solution of Solid Substances in Their Own Solutions. *J. Am. Chem. Soc.*, **1897**. *19*(12): p. 930-934.

50.Berthoud, A.L., Journal De Chimique Physique **1912**. *10*: p. 624.

51.Valeton, J., I. Wachstum Und Auflösung Der Kristalle. Iii. *Zeitschrift für Kristallographie-Crystalline Materials*, **1924**. *60*(1-6): p. 1-38.

52.Englezos, P., Kalogerakis, N., Dholabhai, P., and Bishnoi, P., Kinetics of Formation of Methane and Ethane Gas Hydrates. *Chem. Eng. Sci.*, **1987**. *42*(11): p. 2647-2658.

53.Malegaonkar, M.B., Dholabhai, P.D., and Bishnoi, P.R., Kinetics of Carbon Dioxide and Methane Hydrate Formation. *The Canadian Journal of Chemical Engineering*, **1997**. *75*(6): p. 1090-1099.

54.Hashemi, S., Macchi, A., and Servio, P., Gas Hydrate Growth Model in a Semibatch Stirred Tank Reactor. *Industrial & Engineering Chemistry Research*, **2007**. *46*(18): p. 5907-5912.

55.Bergeron, S. and Servio, P., CO_2 and Ch 4 Mole Fraction Measurements During Hydrate Growth in a Semi-Batch Stirred Tank Reactor and Its Significance to Kinetic Modeling. *Fluid Phase Equilib.*, **2009**. *276*(2): p. 150-155.

56.Bergeron, S. and Servio, P., Reaction Rate Constant of CO_2 Hydrate Formation and Verification of Old Premises Pertaining to Hydrate Growth Kinetics. *AlChE J.*, **2008**. *54*(11): p. 2964-2970.

57.Bergeron, S., Beltrán, J.G., and Servio, P., Reaction Rate Constant of Methane Clathrate Formation. *Fuel*, **2010**. *89*(2): p. 294-301.

58.Clarke, M.A. and Bishnoi, P., Determination of the Intrinsic Kinetics of CO_2 Gas Hydrate Formation Using in Situ Particle Size Analysis. *Chemical Engineering Science*, **2005**. *60*(3): p. 695-709.

59.Skovborg, P. and Rasmussen, P., A Mass Transport Limited Model for the Growth of Methane and Ethane Gas Hydrates. *Chem. Eng. Sci.*, **1994**. *49*(8): p. 1131-1143.

60.Garcia-Ochoa, F. and Gomez, E., Theoretical Prediction of Gas–Liquid Mass Transfer Coefficient, Specific Area and Hold-up in Sparged Stirred Tanks. *Chem. Eng. Sci.*, **2004**. *59*(12): p. 2489-2501.

61.Uchida, T., Ebinuma, T., Kawabata, J., and Narita, H., Microscopic Observations of Formation Processes of Clathrate-Hydrate Films at an Interface between Water and Carbon Dioxide. *Journal of Crystal Growth*, **1999**. *204*(3): p. 348-356.

62.Mori, Y.H., Estimating the Thickness of Hydrate Films from Their Lateral Growth Rates: Application of a Simplified Heat Transfer Model. *J. Cryst. Growth*, **2001**. *223*(1): p. 206-212.

63.Freer, E.M., Sami Selim, M., and Dendy Sloan Jr, E., Methane Hydrate Film Growth Kinetics. *Fluid Phase Equilibria*, **2001**. *185*(1-2): p. 65-75.

64.Mochizuki, T. and Mori, Y.H., Clathrate-Hydrate Film Growth Along Water/Hydrate-Former Phase Boundaries-Numerical Heat-Transfer Study. *Journal of Crystal Growth*, **2006**. *290*(2): p. 642-652.

65.Bollavaram, P., Devarakonda, S., Selim, M., and Sloan, E., Growth Kinetics of Single Crystal Sii Hydrates: Elimination of Mass and Heat Transfer Effects. *Ann. N.Y. Acad. Sci.*, **2000**. *912*(1): p. 533-543.

66.Shi, B.-H., Gong, J., Sun, C.-Y., Zhao, J.-K., Ding, Y., and Chen, G.-J., An Inward and Outward Natural Gas Hydrates Growth Shell Model Considering Intrinsic Kinetics, Mass and Heat Transfer. *Chem. Eng. J.*, **2011**. *171*(3): p. 1308-1316.

67.Neto, E.T., Rahman, M., Imtiaz, S., dos Santos Pereira, T., and de Sousa, F.S., Coupled Heat and Mass Transfer Cfd Model for Methane Hydrate, in ASME 2015 34th International Conference on Ocean, Offshore and Arctic Engineering; American Society of Mechanical Engineers:2015.

68.Odukoya, A. and Naterer, G.F., Heat Transfer and Multiphase Flow with Hydrate Formation in Subsea Pipelines. *Heat Mass Transfer.*, **2015**. *51*(7): p. 901-909.

69.Larsen, R., Knight, C.A., and Sloan Jr, E.D., Clathrate Hydrate Growth and Inhibition. *Fluid Phase Equilib.*, **1998**. *150–151*: p. 353-360.

70.Lekvam, K. and Ruoff, P., A Reaction Kinetic Mechanism for Methane Hydrate Formation in Liquid Water. *Journal of the American Chemical Society*, **1993**. *115*(19): p. 8565-8569.

71.Meindinyo, R.-E.T., Svartaas, T.M., Nordbø, T.N., and Bøe, R., Gas Hydrate Growth Estimation Based on Heat Transfer. *Energy & Fuels*, **2015**. *29*(2): p. 587-594.

72.Xie, Y., Guo, K., Liang, D., Fan, S., and Gu, J., Steady Gas Hydrate Growth Along Vertical Heat Transfer Tube without Stirring. *Chem. Eng. Sci.*, **2005**. *60*(3): p. 777-786.

73.Clarke, M. and Bishnoi, P.R., Determination of the Activation Energy and Intrinsic Rate Constant of Methane Gas Hydrate Decomposition. *The Canadian Journal of Chemical Engineering*, **2001**. *79*(1): p. 143-147.

74.Roosta, H., Khosharay, S., and Varaminian, F., Experimental Study of Methane Hydrate Formation Kinetics with or without Additives and Modeling Based on Chemical Affinity. *Energy Convers. Manage.*, **2013**. *76*: p. 499-505.

75.Takahata, M., Kashiwaya, Y., and Ishii, K., Kinetics of Methane Hydrate Formation Catalyzed by Iron Oxide and Carbon under Intense Stirring Conditions. *Materials transactions*, **2010**. *51*(4): p. 727-734.

76.Daraboina, N., Linga, P., Ripmeester, J., Walker, V.K., and Englezos, P., Natural Gas Hydrate Formation and Decomposition in the Presence of Kinetic Inhibitors. 2. Stirred Reactor Experiments. *Energy & Fuels*, **2011**. *25*(10): p. 4384-4391.

77.Abay, H.K. and Svartaas, T.M., Effect of Ultralow Concentration of Methanol on Methane Hydrate Formation. *Energy & Fuels*, **2009**. *24*(2): p. 752-757.

78.Abay, H.K. and Svartaas, T.M., Multicomponent Gas Hydrate Nucleation: The Effect of the Cooling Rate and Composition. *Energy & Fuels*, **2010**. *25*(1): p. 42-51.

79.Abay, H.K., Svartaas, T.M., and Ke, W., Effect of Gas Composition on Sii Hydrate Growth Kinetics. *Energy & Fuels*, **2011**. *25*(4): p. 1335-1341.

80.Barker, J. and Gomez, R., Formation of Hydrates During Deepwater Drilling Operations. *Journal of Petroleum Technology*, **1989**. *41*(03): p. 297-301.

81.Zamora, M., Broussard, P., and Stephens, M., The Top 10 Mud-Related Concerns in Deepwater Drilling Operations, in SPE International Petroleum Conference and Exhibition in Mexico; Society of Petroleum Engineers:2000.

82.Gbaruko, B., Igwe, J., Gbaruko, P., and Nwokeoma, R., Gas Hydrates and Clathrates: Flow Assurance, Environmental and Economic Perspectives and the Nigerian Liquified Natural Gas Project. *Journal of Petroleum Science and Engineering*, **2007**. *56*(1): p. 192-198.

83.Fisher, R., Hall, S.J., Cam, J.-F., and De La Porte, D., Field Deployment of the World's First Electrically Trace Heated Pipe in Pipe, in Offshore Technology Conference; Offshore Technology Conference:2012.

84.Lervik, J.K., Hoyer-Hansen, M., Iversen, Ø., and Nilsson, S., New Developments of Direct Electrical Heating for Flow Assurance, in The Twenty-second International Offshore and Polar Engineering Conference; International Society of Offshore and Polar Engineers:2012.

85.Roth, R.F., Voight, R., and DeGeer, D., Direct Electrical Heating (Deh) Provides New Opportunities for Arctic Pipelines, in OTC Arctic Technology Conference; Offshore Technology Conference:2012.

86.Solheim, K.T. and Nysveen, A., Hydrate Management of Jumpers by Electrical Heating, in The Twenty-fourth International Ocean and Polar Engineering Conference; International Society of Offshore and Polar Engineers:2014.

87.Wilson, A., World's Longest Electrically Heated Flowline Allows Hp/Ht Field Tieback to Existing Host. *Journal of Petroleum Technology*, **2013**. *65*(02): p. 109-112.

88.Mokhatab, S., Wilkens, R., and Leontaritis, K., A Review of Strategies for Solving Gas-Hydrate Problems in Subsea Pipelines. *Energy Sources, Part A*, **2007**. *29*(1): p. 39-45.

89.Kelland, M.A., History of the Development of Low Dosage Hydrate Inhibitors. *Energy & Fuels*, **2006**. *20*(3): p. 825-847.

90.Freij-Ayoub, R., Tan, C., Clennell, B., Tohidi, B., and Yang, J., A Wellbore Stability Model for Hydrate Bearing Sediments. *Journal of Petroleum Science and Engineering*, **2007**. *57*(1): p. 209-220.

91.Tan, C.P., Freij-Ayoub, R., Clennell, M.B., Tohidi, B., and Yang, J., Managing Wellbore Instability Risk in Gas Hydrate-Bearing Sediments, in SPE Asia Pacific Oil and Gas Conference and Exhibition; Society of Petroleum Engineers:2005.

92.Hovland, M. and Gudmestad, O.T., Potential Influence of Gas Hydrates on Seabed Installations. *Washington DC American Geophysical Union Geophysical Monograph Series*, **2001**. *124*: p. 307-315.

93.Ruppel, C., Boswell, R., and Jones, E., Scientific Results from Gulf of Mexico Gas Hydrates Joint Industry Project Leg 1 Drilling: Introduction and Overview. *Marine and Petroleum Geology*, **2008**. *25*(9): p. 819-829.

94.Bohrmann, G., Greinert, J., Suess, E., and Torres, M., Authigenic Carbonates from the Cascadia Subduction Zone and Their Relation to Gas Hydrate Stability. *Geology*, **1998**. *26*(7): p. 647-650.

95.Dickens, G.R. and Quinby-Hunt, M.S., Methane Hydrate Stability in Seawater. *Geophysical Research Letters*, **1994**. *21*(19): p. 2115-2118.

96.Kvenvolden, K.A., Gas Hydrates as a Potential Energy Resource-a Review of Their Methane Content. *United States Geological Survey, Professional Paper;(United States)*, **1993**. *1570*.

97.Boswell, R. and Collett, T., The Gas Hydrates Resource Pyramid. *Natural Gas & Oil*, **2006**. *304*: p. 285-4541.

98.Holder, G., Kamath, V., and Godbole, S., The Potential of Natural Gas Hydrates as an Energy Resource. *Annual Review of Energy*, **1984**. *9*(1): p. 427-445.

99.Moridis, G., Numerical Studies of Gas Production from Methane Hydrates, in SPE Gas Technology Symposium; Society of Petroleum Engineers:2002.

100.Moridis, G.J., Toward Production from Gas Hydrates: Current Status, Assessment of Resources, and Simulation-Based Evaluation of Technology and Potential. *Lawrence Berkeley National Laboratory*, **2008**.

101.Pooladi-Darvish, M., Gas Production from Hydrate Reservoirs and Its Modeling. *Journal of Petroleum Technology*, **2004**. *56*(06): p. 65-71.

102.Dallimore, S., Collett, T., Uchida, T., Weber, M., Takahashi, H., and Mroz, T., *Overview of Gas Hydrate Research at the Mallik Field in the*

Mackenzie Delta, Northwest Territories, Canada. 2002, National Energy Technology Laboratory.

103.*Mallik 2002 Gas Hydrate Production Well Program*.

104.USGS, *International Gas Hydrate Research - March 2014*.

105.Stevens, J.C., Howard, J.J., Baldwin, B.A., Ersland, G., Husebø, J., and Graue, A., Experimental Hydrate Formation and Gas Production Scenarios Based on CO_2 Sequestration, in Proceedings of the 6th International Conference on Gas Hydrates:2008.

106.Graue, A., Kvamme, B., Baldwin, B., Stevens, J., Howard, J., Aspenes, E., Ersland, G., Husebø, J., and Zornes, D., Environmentally Friendly CO_2 Storage in Hydrate Reservoirs Benefits from Associated Spontaneous Methane Production, in Offshore Technology Conference; Offshore Technology Conference:2006.

107.Ohgaki, K., Takano, K., Sangawa, H., Matsubara, T., and Nakano, S., Methane Exploitation by Carbon Dioxide from Gas Hydrates. Phase Equilibria for CO_2-Ch4 Mixed Hydrate System. *J. Chem. Eng. Jpn.*, **1996**. *29*(3): p. 478-483.

108.Jadhawar, P., Yang, J., Jadhawar, J., and Tohidi, B., Preliminary Experimental Investigation on Replacing Methane in Hydrate Structure with Carbon Dioxide in Porous Media, in Proceedings of the Fifth International Conference on Gas Hydates:2005.

109.Herzog, H. and Golomb, D., Carbon Capture and Storage from Fossil Fuel Use. *Encyclopedia of energy*, **2004**. *1*: p. 1-11.

110.Kvamme, B., Feasibility of Simultaneous CO_2 Storage and Ch4 Production from Natural Gas Hydrate Using Mixtures of CO_2 and N_2. *Can. J. Chem.*, **2015**. *93*(8): p. 897-905.

111.Uchida, T., Ikeda, I.Y., Takeya, S., Kamata, Y., Ohmura, R., Nagao, J., Zatsepina, O.Y., and Buffett, B.A., Kinetics and Stability of CH_4– CO_2 Mixed Gas Hydrates During Formation and Long-Term Storage. *ChemPhysChem*, **2005**. *6*(4): p. 646-654.

112. Yang, M., Song, Y., Jiang, L., Zhu, N., Liu, Y., Zhao, Y., Dou, B., and Li, Q., CO_2 Hydrate Formation and Dissociation in Cooled Porous Media: A Potential Technology for CO_2 Capture and Storage. *Environmental science & technology*, **2013**. *47*(17): p. 9739-9746.

113. Husebø, J., Ersland, G., Graue, A., and Kvamme, B., Effects of Salinity on Hydrate Stability and Implications for Storage of CO_2 in Natural Gas Hydrate Reservoirs. *Energy Procedia*, **2009**. *1*(1): p. 3731-3738.

114. Jemai, K., Kvamme, B., and Vafaei, M.T., Theoretical Studies of CO_2 Hydrates Formation and Dissociation in Cold Aquifers Using Retrasocodebright Simulator. *Reactive transport modelling of hydrate phase transition dynamics in porous media*, **2014**.

115. Kvamme, B., Baig, K., Qasim, M., and Bauman, J., Thermodynamic and Kinetic Modeling of CH_4/CO_2 Hydrates Phase Transitions. *International Journal of Energy and Environment*, **2013**. *7*: p. 1-8.

116. Vafaei, M.T., Kvamme, B., Chejara, A., and Jemai, K., Nonequilibrium Modeling of Hydrate Dynamics in Reservoir. *Energy & Fuels*, **2012**. *26*(6): p. 3564-3576.

117. Gudmundsson, J.S., *Method for Production of Gas Hydrates for Transportation and Storage*. 1996, Google Patents.

118. Gudmundsson, J.S., Parlaktuna, M., and Khokhar, A., Storage of Natural Gas as Frozen Hydrate. *SPE Production & Facilities*, **1994**. *9*(01): p. 69-73.

119. Babu, P., Linga, P., Kumar, R., and Englezos, P., A Review of the Hydrate Based Gas Separation (Hbgs) Process for Carbon Dioxide Pre-Combustion Capture. *Energy*, **2015**. *85*: p. 261-279.

120. Anderson, G.K., Enthalpy of Dissociation and Hydration Number of Methane Hydrate from the Clapeyron Equation. *The Journal of Chemical Thermodynamics*, **2004**. *36*(12): p. 1119-1127.

121. Huo, Z., Freer, E., Lamar, M., Sannigrahi, B., Knauss, D., and Sloan, E., Hydrate Plug Prevention by Anti-Agglomeration. *Chem. Eng. Sci.*, **2001**. *56*(17): p. 4979-4991.

122.Østergaard, K.K., Tohidi, B., Burgass, R.W., Danesh, A., and Todd, A.C., Hydrate Equilibrium Data of Multicomponent Systems in the Presence of Structure-Ii and Structure-H Heavy Hydrate Formers. *Journal of Chemical & Engineering Data*, **2001**. *46*(3): p. 703-708.

123.Taylor, C.J., Miller, K.T., Koh, C.A., and Sloan, E.D., Macroscopic Investigation of Hydrate Film Growth at the Hydrocarbon/Water Interface. *Chem. Eng. Sci.*, **2007**. *62*(23): p. 6524-6533.

124.Herri, J.-M., Gruy, F., Pic, J.-S., Cournil, M., Cingotti, B., and Sinquin, A., Interest of in Situ Turbidimetry for the Characterization of Methane Hydrate Crystallization: Application to the Study of Kinetic Inhibitors. *Chem. Eng. Sci.*, **1999**. *54*(12): p. 1849-1858.

125.Dorstewitz, F. and Mewes, D., The Influence of Hydrate Formation on Heat Transfer in Gas Pipelines, in International Symposium on Transport Phenomena in Thermal Engineering 1993 년 제 2 권:1993.

126.Mochizuki, T. and Mori, Y.H., Clathrate-Hydrate Film Growth Along Water/Hydrate-Former Phase Boundaries—Numerical Heat-Transfer Study. *J. Cryst. Growth*, **2006**. *290*(2): p. 642-652.

127.Handa, Y., Compositions, Enthalpies of Dissociation, and Heat Capacities in the Range 85 to 270 K for Clathrate Hydrates of Methane, Ethane, and Propane, and Enthalpy of Dissociation of Isobutane Hydrate, as Determined by a Heat-Flow Calorimeter. *The Journal of Chemical Thermodynamics*, **1986**. *18*(10): p. 915-921.

128.Gupta, A., Lachance, J., Sloan, E., and Koh, C.A., Measurements of Methane Hydrate Heat of Dissociation Using High Pressure Differential Scanning Calorimetry. *Chem. Eng. Sci.*, **2008**. *63*(24): p. 5848-5853.

129.Bergman, T.L., Incropera, F.P., DeWitt, D.P., and Lavine, A.S., *Fundamentals of Heat and Mass Transfer*. John Wiley & Sons,2011.

130.Lekvam, K. and Bishnoi, P.R., Dissolution of Methane in Water at Low Temperatures and Intermediate Pressures. *Fluid Phase Equilib.*, **1997**. *131*(1): p. 297-309.

131.Peng, B., Dandekar, A., Sun, C., Luo, H., Ma, Q., Pang, W., and Chen, G., Hydrate Film Growth on the Surface of a Gas Bubble Suspended in Water. *J. Phy. Chem. B*, **2007**. *111*(43): p. 12485-12493.

132.Happel, J., Hnatow, M.A., and Meyer, H., The Study of Separation of Nitrogen from Methane by Hydrate Formation Using a Novel Apparatusa. *Ann. N.Y. Acad. Sci.*, **1994**. *715*(1): p. 412-424.

133.Arjmandi, M., Tohidi, B., Danesh, A., and Todd, A.C., Is Subcooling the Right Driving Force for Testing Low-Dosage Hydrate Inhibitors? *Chem. Eng. Sci.*, **2005**. *60*(5): p. 1313-1321.

134.Joshi, S.V., Grasso, G.A., Lafond, P.G., Rao, I., Webb, E., Zerpa, L.E., Sloan, E.D., Koh, C.A., and Sum, A.K., Experimental Flowloop Investigations of Gas Hydrate Formation in High Water Cut Systems. *Chem. Eng. Sci.*, **2013**. *97*: p. 198-209.

135.Chaudhari, R., Gholap, R., Emig, G., and Hofmann, H., Gas-Liquid Mass Transfer in "Dead-End" Autoclave Reactors. *Can. J. Chem. Eng.*, **1987**. *65*(5): p. 744-751.

136.Yang, S., Li, X., Yang, C., Ma, B., and Mao, Z.-S., Computational Fluid Dynamics Simulation and Experimental Measurement of Gas and Solid Holdup Distributions in a Gas–Liquid–Solid Stirred Reactor. *Ind. Eng. Chem. Res.*, **2015**. *55*(12): p. 3276-3286.

137.Ke, W. and Svartaas, T.M., Effects of Stirring and Cooling on Methane Hydrate Formation in a High-Pressure Isochoric Cell, in Proceedings of the 7th International Conference on Gas Hydrates, Edinburgh, Scotland, United Kingdom, July 17-21 2011:2011.

138.Høvring, E., On the Activation Energy for the Formation of a Critical Size Water Cluster in Structure I and Structure Ii Gas Hydrates. **2012**.

139.Kvamme, B., Kinetics of Hydrate Formation from Nucleation Theory. *Int. J. Offshore Polar Eng.*, **2002**. *12*(04).

140.Tatterson, G.B., *Fluid Mixing and Gas Dispersion in Agitated Tanks*. McGraw-Hill Companies,1991.

141.Mori, Y.H., On the Scale-up of Gas-Hydrate-Forming Reactors: The Case of Gas-Dispersion-Type Reactors. *Energies*, **2015**. *8*(2): p. 1317-1335.

142.Bhavaraju, S.M., Russell, T., and Blanch, H., The Design of Gas Sparged Devices for Viscous Liquid Systems. *AlChE J.*, **1978**. *24*(3): p. 454-466.

143.Nauman, E.B., *Chemical Reactor Design, Optimization, and Scaleup*. John Wiley & Sons,2008.

144.Manglik, R.M. and Bergles, A.E., Swirl Flow Heat Transfer and Pressure Drop with Twisted-Tape Inserts. *Advances in heat transfer*, **2003**. *36*: p. 183-266.

145.Adeyemo, A., Kumar, R., Linga, P., Ripmeester, J., and Englezos, P., Capture of Carbon Dioxide from Flue or Fuel Gas Mixtures by Clathrate Crystallization in a Silica Gel Column. *International Journal of Greenhouse Gas Control*, **2010**. *4*(3): p. 478-485.

146.Park, S., Lee, S., Lee, Y., Lee, Y., and Seo, Y., Hydrate-Based Pre-Combustion Capture of Carbon Dioxide in the Presence of a Thermodynamic Promoter and Porous Silica Gels. *Int. J. Greenhouse Gas Control*, **2013**. *14*: p. 193-199.

147.Seo, Y.-T., Moudrakovski, I.L., Ripmeester, J.A., Lee, J.-w., and Lee, H., Efficient Recovery of CO_2 from Flue Gas by Clathrate Hydrate Formation in Porous Silica Gels. *Environmental science & technology*, **2005**. *39*(7): p. 2315-2319.

148.Yang, M., Song, Y., Jiang, L., Wang, X., Liu, W., Zhao, Y., Liu, Y., and Wang, S., Dynamic Measurements of Hydrate Based Gas Separation in Cooled Silica Gel. *Journal of Industrial and Engineering Chemistry*, **2014**. *20*(1): p. 322-330.

149.Brown, T.D., Taylor, C.E., and Bernardo, M.P., Rapid Gas Hydrate Formation Processes: Will They Work? *Energies*, **2010**. *3*(6): p. 1154-1175.

150.Kennicutt II, M.C., Brooks, J.M., and Cox, H.B., *The Origin and Distribution of Gas Hydrates in Marine Sediments*, in *Organic Geochemistry*. 1993, Springer. p. 535-544.

151.Waseda, A., Organic Carbon Content, Bacterial Methanogenesis, and Accumulation Processes of Gas Hydrates in Marine Sediments. *Geochem. J.*, **1998**. *32*(3): p. 143-157.

152.Kvenvolden, K.A., Methane Hydrate—a Major Reservoir of Carbon in the Shallow Geosphere? *Chem. Geol.*, **1988**. *71*(1-3): p. 41-51.

153.Sloan, E.D., Gas Hydrates: Review of Physical/Chemical Properties. *Energy & Fuels*, **1998**. *12*(2): p. 191-196.

154.Schmidt, E. and Grigull, U., Properties of Water and Steam in Si-Units. 4. **1989**.

155.Winters William, J., Pecher Ingo, A., Waite William, F., and Mason David, H., *Physical Properties and Rock Physics Models of Sediment Containing Natural and Laboratory-Formed Methane Gas Hydrate*, in *American Mineralogist*. 2004. p. 1221.

156.Liu, B., Pang, W., Peng, B., Sun, C., and Chen, G., Heat Transfer Related to Gas Hydrate Formation/Dissociation. *Developments in Heat Transfer*, **2010**: p. 477-502.

157.Waite, W.F., Stern, L.A., Kirby, S., Winters, W.J., and Mason, D., Simultaneous Determination of Thermal Conductivity, Thermal Diffusivity and Specific Heat in Si Methane Hydrate. *Geophysical Journal International*, **2007**. *169*(2): p. 767-774.

158.HUANG, D.Z., FAN, S.S., LIANG, D.Q., and FENG, Z.P., Gas Hydrate Formation and Its Thermal Conductivity Measurement. *Chinese Journal of Geophysics*, **2005**. *48*(5): p. 1201-1207.

159.Austvik, T., Li, X., and Gjertsen, L.H., Hydrate Plug Properties: Formation and Removal of Plugs. *Ann. N.Y. Acad. Sci.*, **2000**. *912*(1): p. 294-303.

160.Engeskaug, R., Thorbjørnsen, E., and Svendsen, H.F., Wall Heat Transfer in Stirred Tank Reactors. *Ind. Eng. Chem. Res.*, **2005**. *44*(14): p. 4949-4958.

161.Debab, A., Chergui, N., Bekrentchir, K., and Bertrand, J., An Investigation of Heat Transfer in a Mechanically Agitated Vessel. *J. Appl. Fluid Mec.*, **2011**. *4*(2): p. 43-50.

162.Meindinyo, R.-E.T., Bøe, R., Svartås, T.M., and Bru, S., Experimental Study on the Effect of Gas Hydrate Content on Heat Transfer, in ASME 2015 34th International Conference on Ocean, Offshore and Arctic Engineering; American Society of Mechanical Engineers:2015.

163.Andersson, V. and Gudmundsson, J.S., Flow Properties of Hydrate-in-Water Slurries. *Ann. N.Y. Acad. Sci.*, **2000**. *912*(1): p. 322-329.

Part II – Papers

Paper I

Heat Transfer During Hydrate Formation - An Investigation on the Effect of Hydrate Content on the Heat Transfer Coefficient of Gas Hydrate Slurry

Published in:
Proceedings of the 8th International Conference on Gas Hydrates (ICGH8-2014), Beijing, China, 28 July - 1 August, 2014.

Paper II

A Parametric Study of Hydrate Growth Behaviour

Published in:
Proceedings of the 8th International Conference on Gas Hydrates (ICGH8-2014), Beijing, China, 28 July - 1 August, 2014.

Paper III

Gas hydrate growth estimation based on heat transfer.

Published in:
Energy & Fuels, **2015**, 29.2: 587-594.

Paper IV

Experimental Study on the Effect of Gas Hydrate Content on Heat Transfer.

Published in:
ASME 2015 34th International Conference on Ocean, Offshore and Arctic Engineering. American Society of Mechanical Engineers, **2015**.

Not available in UiS Brage due to copyright

Paper V

Gas Hydrate Growth Kinetics: A Parametric Study.

Published in:
Energies 9.12 (2016): 1021.

Not available in UiS Brage due to copyright.

Read the paper here:

http://www.mdpi.com/1996-1073/9/12/1021

Paper VI

Intermolecular Forces in Clathrate hydrate related processes.

Published in:
ASME 2015 34th International Conference on Ocean, Offshore and Arctic Engineering. American Society of Mechanical Engineers, **2015**.